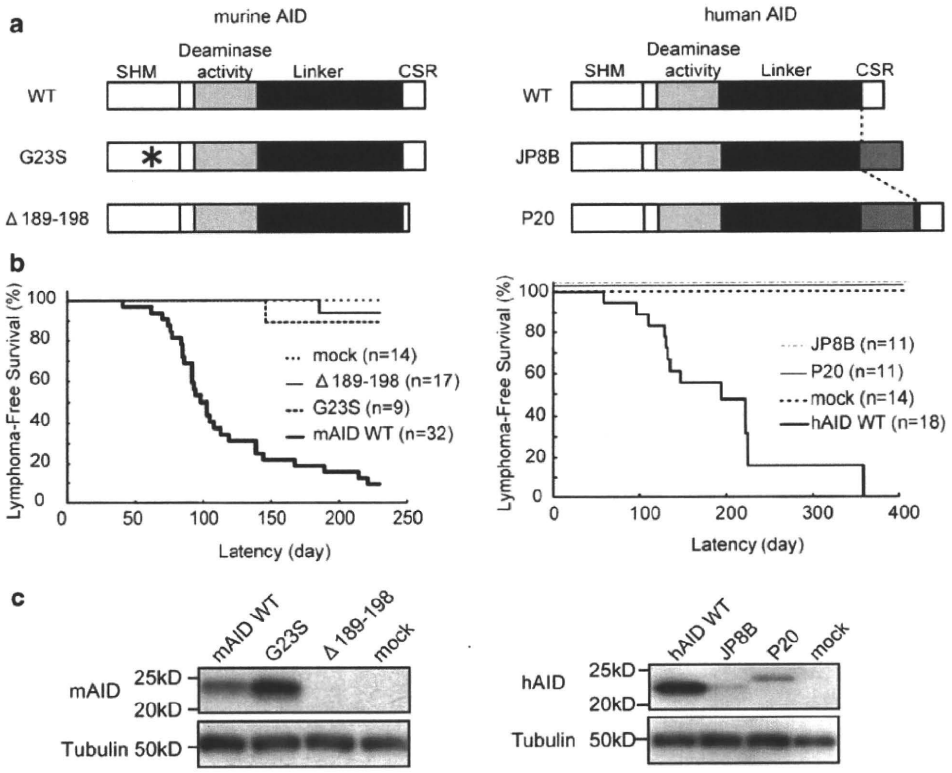

Figure 2 A BMT model using mutant forms of AID. (**a**) Diagrams of WT or mutant forms of AID. Left panel, mAID. G23S harbors a missense mutation (asterisk). Δ189–198 mutant lacks C-terminal 10 residues. Right panel, human AID (hAID). JP8B has a frameshift replacement of the C-terminus with 26 residues. P20 has an insertion of 34 residues. (**b**) Kaplan–Meier curves for the survival. Left panel, mAID. Right panel, hAID. (**c**) Expression of WT or mutant forms of AID in GFP-sorted BM cells by western blotting. Left panel, mAID. Right panel, hAID.

activity (Figure 2a, left panel).[5] Interestingly, recipients of these mutants showed a significantly decreased incidence of lymphoma as compared with those of WT (G23S $n=1/9$, 11%; Δ189–198 $n=1/17$, 6%) (Figure 2b, left panel). Each mutant developed only T-lymphoma. The expression level of G23S was comparable with that of WT in GFP-sorted BM cells (Figure 2c, left panel). On the other hand, the expression of Δ189–198 mutant in GFP-sorted BM cells was hardly detectable (Figure 2c, left panel). Similar results were obtained when hAID and its C-terminal mutants JP8B and P20 were transduced into BM cells (Figures 2a–c, right panels). Therefore, it was difficult to evaluate the effect of the CSR activity of AID on lymphomagenesis. Altogether, these results suggest that the intact form of AID with SHM activity is required to maximally exert its oncogenic activity.

An active mutation of K-ras in one case as well as multiple point mutations of Notch1, PTEN, and c-Myc was observed in AID-induced T-lymphoma

As point mutations are introduced into non-Ig genes such as *TCR* or *c-Myc* gene in T-lymphoma cells of AID-Tg mice,[13] we next asked which mutations caused by AID were responsible for T-lymphomagenesis in a mouse BMT model. On the basis of the fact that AID-mediated mutations occur after about 100 nucleotides downstream of the promoter and extend to 1–2 kb,[24] we performed genomic sequencing of several possible target genes in the region encompassing 0.5–1 kb from the transcription start site, in addition to the mutational hotspots implicated in tumorigenesis (Supplementary Table 3 and data not shown). Similar to the results on AID-Tg mice,[13] multiple mutations were observed in the *c-Myc* gene. An activating mutation of *K-ras* (G13D) was detected in 1 out of 14 analyzed samples, although no mutation was found in *N-ras*, *H-ras*, or *p53* tumor suppressor gene. As for genes involved in human T-ALL, *Notch1*[25] and *Pten*, but not *Fbxw7*, had multiple mutations. Intriguingly, we found several mutations in exon 27 (HD domain) and exon 34 (PEST domain), mutational hotspots of *Notch1* far downstream from the transcription start site. Consistent with the earlier report,[13] detected mutations were predominantly transition mutations and strongly biased to GC bases. Collectively, multiple mutations in T-lymphoma were introduced by AID, probably in association with lymphomagenesis.

Most AID-induced T-lymphoma cells exhibited constitutive activation of Notch1 and were susceptible to a γ-secretase inhibitor

The finding that Notch1 mutations were observed in AID-induced T-lymphoma led us to address the question of whether these mutations caused the activation of Notch1, leading to T-lymphomagenesis. Interestingly, western blot analysis demonstrated that cleavage of intracellular Notch1 (ICN) was evident in most T-lymphoma samples tested (Figure 3a), indicating that constitutive activation of Notch1 occurred in most T-lymphoma cells. In support of this finding, real-time PCR analysis showed increased expression of Hes1 and c-Myc and decreased expression of PTEN in most samples (Figure 3b). Expression levels of Notch1 did not significantly vary among these samples, except for a few cases. Interestingly, when we treated two cell

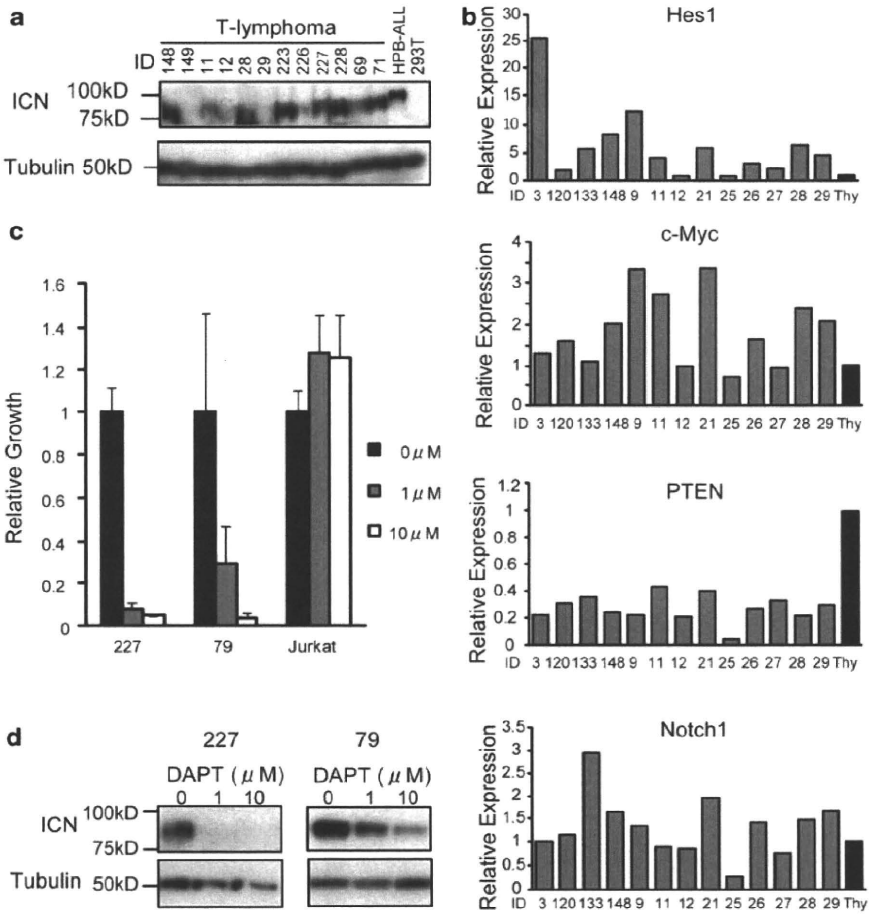

Figure 3 Notch1 is constitutively activated in AID-induced T-lymphoma. (**a**) Cleavage of intracellular Notch1 (ICN) in AID-induced T-lymphoma confirmed by western blotting. (**b**) Relative expression levels of Hes1, c-Myc, PTEN, or Notch1 in T-lymphoma samples and normal thymocytes (Thy) measured by real-time PCR. (**c**) The relative growth estimated by colorimetric assay. Two cell lines 227 and 79 established from AID-induced T-lymphoma, or Jurkat cells were treated with indicated concentrations of DAPT for 72 h. The means ± s.d. of triplicate measurements are shown. Data are representative of three independent experiments. (**d**) Cleavage of ICN examined by western blotting. Cells were treated as described in (**c**). Data are representative of three independent experiments.

lines established from AID-induced T-lymphoma with a γ-secretase inhibitor, DAPT, the growth as well as the cleavage of ICN of these cell lines was dose dependently inhibited by DAPT (Figures 3c and d). Although Notch1 mutations did not account for constitutive activation of Notch1 in all cases, these results indicated that T-lymphomagenesis in most cases was induced by Notch1 activation, probably in conjunction with AID-introduced mutations of the related genes.

Truncation mutations of Ebf1 and Pax5 were found in AID-induced B-lymphoma

To investigate the relevant mechanism of AID-induced B-lymphomagenesis, we performed genomic sequencing of the *Ebf1* and *Pax5* genes of AID-induced B-leukemia/lymphoma of seven recipient mice (Supplementary Table 4 and data not shown). Intriguingly, sequencing of *Ebf1* revealed a 23-base deletion and a 4-base insertion in exon 2, which together resulted in truncation in one sample. In addition, multiple point mutations were found in three samples. As for *Pax5*, we found a truncation caused by a couple of 2-base deletions and a point mutation in exon 1a in one case, and point mutations in two cases. On the basis of the recent study,[26] the aberrations of *Pax5* and *Ebf1* genes described above might have some function in B-lymphomagenesis in the recipient mice. On the other hand, we did not find c-Myc/IgH chromosomal translocations in B-lymphoma samples analyzed by PCR combined with Southern blotting (data not shown).[27] Collectively, these results suggested that B-lymphomagenesis in a BMT model was, at least in part, due to AID-introduced mutations/deletions of the genes regulating B-cell differentiation.

Discussion

In this study, we constructed a mouse BMT model to test whether AID is implicated in the pathogenesis of leukemia/lymphoma including myeloid leukemia. Our results revealed that aberrant expression of AID in BM cells led to T-lymphoma and less frequently B-leukemia/lymphoma, but not myeloid leukemia (Figure 1). The recipient mice developed 'thymic' T-lymphoma, but not 'peripheral type' T-lymphoma observed in 65% of AID-Tg mice.[13] It was noteworthy that B-leukemia/lymphoma was observed in our BMT model, but not in AID-Tg

mice,[13,15,28] because AID is implicated in the pathogenesis of human B-cell malignancy.[6–9] Interestingly, nude mice developed only B-leukemia when used as recipients, probably due to lack of thymus (Supplementary Figure 3). The differences between AID-Tg mice and the BMT model were probably caused by the expression levels in the different types of cells, although we could not completely exclude the possibility that RIS affected the phenotypes. We have two hypotheses for AID-induced lymphomagenesis in the BMT model: (1) AID-transduced stem/progenitor cells may move to thymus, where they would be susceptible to AID-mediated mutations and rapidly acquire oncogenic properties at an early stage of T-lineage development; (2) AID could introduce some mutations and transform cells at stem/progenitor levels, which would commit to T-lineage in thymus. Otherwise, AID-transduced stem/progenitor cells would be transformed during the early B-lineage development in BM and spleen, which result in B-leukemia/lymphoma. Both hypotheses would explain why no lymphoma was observed in AID-Tg mice with its expression restricted to mature lymphocytes.[15,28] However, it is not clear why AID overexpression did not induce myeloid leukemia. We found scarcely detectable levels of AID in human myeloid malignancy (Supplementary Figure 4). Recent study showed that chronic myeloid leukemia (CML) does not express AID unless CML cells are forced into B-lineage conversion by Pax5.[9] It is possible that the protective machinery efficiently works against AID functioning as a mutator in myeloid cells, but not in lymphoid cells. Indeed, we confirmed that AID overexpression did not affect myeloid cell development in BM one month after transplantation (data not shown). In addition, sorted myeloid progenitors (common myeloid progenitors and granulocyte-macrophage progenitors) transduced with AID did not cause myeloid leukemia in our BMT model (data not shown). According to the recent studies, the balance between error-prone repair (EPR) and high-fidelity repair (HFR) determines the outcome of AID-generated uracils, that is, accumulation or elimination of mutations.[29] It is tempting to speculate that the frequencies of uracils generated by AID are not different between the myeloid- and lymphoid-lineage, but that HFR overcomes EPR in the myeloid-lineage. In any case, solving the riddle of how AID induces leukemia/lymphoma in a cell-lineage–dependent manner will help understand AID functions.

It is generally accepted that the N-terminal or C-terminal domain of AID is important for SHM or CSR activity, respectively,[3–5] but neither activity is regulated in an exclusively distinct way. Our results showed that AID mutants with decreased SHM or CSR activity have impaired oncogenic activity (Figure 2). It must be noted that expression levels of mouse mutant Δ189–198 as well as human mutants JP8B and P20 in GFP-sorted BM cells were lower than those of WTs, possibly due to protein instability of these C-terminal mutants.[30] Therefore, we cannot answer the question whether CSR activity is indispensable for oncogenicity of AID, but we assume that the maximum ability of AID to cause lymphoma requires an intact form of AID with SHM activity.

We clarified to some extent the mechanism by which AID-introduced mutations of tumor-related genes led to lymphomagenesis (Supplementary Table 3). As reported on AID-Tg mice,[13] multiple mutations of the *c-Myc* gene were found in T-lymphoma samples. The *Notch1* gene was mutated in exon 1 and mutational hotspots (HD and PEST domains) in four cases. Intriguingly, Notch1 was constitutively activated in T-lymphoma more frequently than expected from the mutation frequency of *Notch1* (Figure 3). We speculate that AID-mediated mutations of other genes caused secondary Notch1 activation, resulting in T-lymphoma. However, one such candidate, *Fbxw7*,[31] did not have significant mutations. Further examination will identify unknown mutations responsible for human T-lymphoma/leukemia.

Sequencing analysis of AID-induced B-leukemia/lymphoma samples revealed frequent mutations in the *Ebf1* and *Pax5* genes (Supplementary Table 4 and data not shown). Importantly, we found truncation mutations in *Ebf1* and *Pax5* that probably have oncogenic properties; mono-allelic deletions of these genes were observed in human B-ALL.[26] As for chromosomal instability, c-Myc/IgH translocation was not detected (data not shown). The presence of TCR translocations was unlikely, as no chromosomal translocation was detected in AID-induced T-lymphoma observed in AID-Tg mice.[13,15] The present results suggest that, like thymic T-lymphoma, B-leukemia/lymphoma was induced by AID-introduced mutations/deletions of the key molecules regulating B-cell differentiation and/or proliferation.

In conclusion, this is the first report on the potential of AID overexpression to promote B-cell lymphomagenesis. Aberrant expression of AID in bone marrow cells induced leukemia/lymphoma in a cell-lineage–dependent manner, probably because an intact form of AID efficiently introduced mutations into the responsible genes, thereby disrupting normal development of lymphoid progenitors.

Conflict of interest

TK serves as a consultant for R&D Systems.

Acknowledgements

We thank Dr Chiba (Tsukuba University, Ibaraki, Japan) for providing HPB-ALL cell line. We are grateful to Dr Dovie Wylie for her excellent language assistance. This work was supported by grants from the Ministry of Education, Science, Technology, Sports and Culture, Japan to TK.

References

1 Muramatsu M, Sankaranand VS, Anant S, Sugai M, Kinoshita K, Davidson NO *et al*. Specific expression of activation-induced cytidine deaminase (AID), a novel member of the RNA-editing deaminase family in germinal center B cells. *J Biol Chem* 1999; **274**: 18470–18476.
2 Muramatsu M, Kinoshita K, Fagarasan S, Yamada S, Shinkai Y, Honjo T. Class switch recombination and hypermutation require activation-induced cytidine deaminase (AID), a potential RNA editing enzyme. *Cell* 2000; **102**: 553–563.
3 Ta VT, Nagaoka H, Catalan N, Durandy A, Fischer A, Imai K *et al*. AID mutant analyses indicate requirement for class-switch-specific cofactors. *Nat Immunol* 2003; **4**: 843–848.
4 Shinkura R, Ito S, Begum NA, Nagaoka H, Muramatsu M, Kinoshita K *et al*. Separate domains of AID are required for somatic hypermutation and class-switch recombination. *Nat Immunol* 2004; **5**: 707–712.
5 Barreto V, Reina-San-Martin B, Ramiro AR, McBride KM, Nussenzweig MC. C-terminal deletion of AID uncouples class switch recombination from somatic hypermutation and gene conversion. *Mol Cell* 2003; **12**: 501–508.
6 Pasqualucci L, Neumeister P, Goossens T, Nanjangud G, Chaganti RS, Kuppers R *et al*. Hypermutation of multiple proto-oncogenes in B-cell diffuse large-cell lymphomas. *Nature* 2001; **412**: 341–346.
7 Greeve J, Philipsen A, Krause K, Klapper W, Heidorn K, Castle BE *et al*. Expression of activation-induced cytidine deaminase in human B-cell non-Hodgkin lymphomas. *Blood* 2003; **101**: 3574–3580.

8 Smit LA, Bende RJ, Aten J, Guikema JE, Aarts WM, van Noesel CJ. Expression of activation-induced cytidine deaminase is confined to B-cell non-Hodgkin's lymphomas of germinal-center phenotype. *Cancer Res* 2003; **63**: 3894–3898.
9 Klemm L, Duy C, Iacobucci I, Kuchen S, von Levetzow G, Feldhahn N *et al.* The B cell mutator AID promotes B lymphoid blast crisis and drug resistance in chronic myeloid leukemia. *Cancer Cell* 2009; **16**: 232–245.
10 Pasqualucci L, Bhagat G, Jankovic M, Compagno M, Smith P, Muramatsu M *et al.* AID is required for germinal center-derived lymphomagenesis. *Nat Genet* 2008; **40**: 108–112.
11 Takizawa M, Tolarova H, Li Z, Dubois W, Lim S, Callen E *et al.* AID expression levels determine the extent of cMyc oncogenic translocations and the incidence of B cell tumor development. *J Exp Med* 2008; **205**: 1949–1957.
12 Matsumoto Y, Marusawa H, Kinoshita K, Endo Y, Kou T, Morisawa T *et al.* Helicobacter pylori infection triggers aberrant expression of activation-induced cytidine deaminase in gastric epithelium. *Nat Med* 2007; **13**: 470–476.
13 Okazaki IM, Hiai H, Kakazu N, Yamada S, Muramatsu M, Kinoshita K *et al.* Constitutive expression of AID leads to tumorigenesis. *J Exp Med* 2003; **197**: 1173–1181.
14 Morisawa T, Marusawa H, Ueda Y, Iwai A, Okazaki IM, Honjo T *et al.* Organ-specific profiles of genetic changes in cancers caused by activation-induced cytidine deaminase expression. *Int J Cancer* 2008; **123**: 2735–2740.
15 Rucci F, Cattaneo L, Marrella V, Sacco MG, Sobacchi C, Lucchini F *et al.* Tissue-specific sensitivity to AID expression in transgenic mouse models. *Gene* 2006; **377**: 150–158.
16 Muto T, Okazaki IM, Yamada S, Tanaka Y, Kinoshita K, Muramatsu M *et al.* Negative regulation of activation-induced cytidine deaminase in B cells. *Proc Natl Acad Sci USA* 2006; **103**: 2752–2757.
17 Casellas R, Yamane A, Kovalchuk AL, Potter M. Restricting activation-induced cytidine deaminase tumorigenic activity in B lymphocytes. *Immunology* 2009; **126**: 316–328.
18 Morita S, Kojima T, Kitamura T. Plat-E: an efficient and stable system for transient packaging of retroviruses. *Gene Ther* 2000; **7**: 1063–1066.
19 Kitamura T, Koshino Y, Shibata F, Oki T, Nakajima H, Nosaka T *et al.* Retrovirus-mediated gene transfer and expression cloning: powerful tools in functional genomics. *Exp Hematol* 2003; **31**: 1007–1014.
20 Watanabe-Okochi N, Kitaura J, Ono R, Harada H, Harada Y, Komeno Y *et al.* AML1 mutations induced MDS and MDS/AML in a mouse BMT model. *Blood* 2008; **111**: 4297–4308.
21 Ye BH, Chaganti S, Chang CC, Niu H, Corradini P, Chaganti RS *et al.* Chromosomal translocations cause deregulated BCL6 expression by promoter substitution in B cell lymphoma. *EMBO J* 1995; **14**: 6209–6217.
22 Pasqualucci L, Migliazza A, Basso K, Houldsworth J, Chaganti RS, Dalla-Favera R. Mutations of the BCL6 proto-oncogene disrupt its negative autoregulation in diffuse large B-cell lymphoma. *Blood* 2003; **101**: 2914–2923.
23 Mullighan CG, Miller CB, Radtke I, Phillips LA, Dalton J, Ma J *et al.* BCR-ABL1 lymphoblastic leukaemia is characterized by the deletion of Ikaros. *Nature* 2008; **453**: 110–114.
24 Longerich S, Tanaka A, Bozek G, Nicolae D, Storb U. The very 5′ end and the constant region of Ig genes are spared from somatic mutation because AID does not access these regions. *J Exp Med* 2005; **202**: 1443–1454.
25 Aster JC, Pear WS, Blacklow SC. Notch signaling in leukemia. *Annu Rev Pathol* 2008; **3**: 587–613.
26 Mullighan CG, Goorha S, Radtke I, Miller CB, Coustan-Smith E, Dalton JD *et al.* Genome-wide analysis of genetic alterations in acute lymphoblastic leukaemia. *Nature* 2007; **446**: 758–764.
27 Ramiro AR, Jankovic M, Eisenreich T, Difilippantonio S, Chen-Kiang S, Muramatsu M *et al.* AID is required for c-myc/IgH chromosome translocations *in vivo*. *Cell* 2004; **118**: 431–438.
28 Muto T, Okazaki IM, Yamada S, Tanaka Y, Kinoshita K, Muramatsu M *et al.* Negative regulation of activation-induced cytidine deaminase in B cells. *Proc Natl Acad Sci USA* 2006; **103**: 2752–2757.
29 Liu M, Schatz DG. Balancing AID and DNA repair during somatic hypermutation. *Trends Immunol* 2009; **30**: 173–181.
30 Geisberger R, Rada C, Neuberger MS. The stability of AID and its function in class-switching are critically sensitive to the identity of its nuclear-export sequence. *Proc Natl Acad Sci USA* 2009; **106**: 6736–6741.
31 O'Neil J, Grim J, Strack P, Rao S, Tibbitts D, Winter C *et al.* FBW7 mutations in leukemic cells mediate NOTCH pathway activation and resistance to gamma-secretase inhibitors. *J Exp Med* 2007; **204**: 1813–1824.

Supplementary Information accompanies the paper on the Leukemia website (http://www.nature.com/leu)

Int J Hematol (2010) 92:553–555
DOI 10.1007/s12185-010-0676-8

LETTER TO THE EDITOR

Giant granulocytic sarcoma of the vagina concurrent with acute myeloid leukemia with t(8;21)(q22;q22) translocation

Jun Imagawa · Yuka Harada · Tetsumi Yoshida · Akira Sakai · Naomi Sasaki · Akiro Kimura · Hironori Harada

Received: 5 June 2010 / Revised: 20 August 2010 / Accepted: 22 August 2010 / Published online: 10 September 2010

Granulocytic sarcoma (GS) is a localized extramedullary solid tumor consisting of immature myeloid cells [1]. Its occurrence in the female genital tract is rare and mainly in ovary or uterus, and the most frequent symptom of GS in the female genital tract is vaginal bleeding [2, 3]. Here we report an extremely rare case of vaginal GS, noticed by vaginal discharge, concurrent with acute myeloid leukemia (AML).

A previously healthy and unmarried 25-year-old female presented with profuse stinking vaginal discharge. Magnetic resonance imaging (MRI) of the pelvis demonstrated a massive 7.9 cm × 4.4 cm tumor between the posterior vaginal wall and the rectum, with propagation into the vaginal cavity (Fig. 1a). A pathological examination of the vaginal biopsy revealed normal squamous cells of the vagina and diffuse subepithelial infiltrates of medium-sized rounded cells in its stroma (Fig. 1d, e). Immunohistochemistry revealed $CD45^+CD56^+CD3^-CD5^-CD15^-CD20^-CD30^-CD79^-$ (Fig. 1f). The histological and immunological findings were suggestive of NK-cell lymphoma. The patient's blood cell count and laboratory data were normal. Fluorodeoxyglucose-positron emission tomography/computed tomography (FDG-PET/CT) examination and bone marrow aspiration were performed for the clinical staging. The vaginal tumor demonstrated an increased FDG uptake with a standard uptake value (SUV) of 7.6 (Fig. 1b, c). No other region including bone marrow showed pathological FDG uptake. However, bone marrow aspiration showed hypercellular marrow comprised predominantly of myeloblasts with Auer rods (FAB classification, M2). Surface antigens of blast cells were $CD34^+CD13^+CD33^+CD117^+CD4^+CD56^+CD3^-CD19^-CD57^-$. A cytogenetic study of the bone marrow cells revealed the chromosomal abnormality, 46,XX,del(7)(q32),t(8;21)(q22;q22), del(12)(p?). With concern for the vaginal tumor possibly being a GS, additional immunohistochemical studies were performed. The vaginal tumor cells were positive for lysozyme, CD68, and CD34 (Fig. 1g), resulting in the alteration of the diagnosis to GS following AML. Furthermore, an RT-PCR analysis of the *AML1-ETO* fusion gene was positive in both the bone marrow cells and the vaginal tumor tissue (Fig. 1h). Immediately, the patient underwent standard induction chemotherapy with idarubicin (12 mg/m^2 for 3 days) and cytarabine (100 mg/m^2 for 7 days), and achieved complete hematological remission. The vaginal tumor also disappeared and the FDG uptake became negative. After five additional cycles of consolidation therapy including a cycle of high-dose cytarabine, she has been in complete cytogenetical remission for 3 years.

We have shown here the first reported case of giant GS in the vagina presenting with t(8;21) AML. This case is exceptional because vaginal discharge was the first sign of an AML. Several retrospective studies have reported that GS has been found with a relatively higher incidence (9–38%) in patients with t(8;21)(q22;q22) translocation [4, 5]. The majority of these GS cases presenting with t(8;21) AML

J. Imagawa · T. Yoshida · A. Sakai · A. Kimura · H. Harada (✉)
Department of Hematology and Oncology, Research Institute for Radiation Biology and Medicine, Hiroshima University, 1-2-3 Kasumi, Miniami-ku, Hiroshima 734-8553, Japan
e-mail: herf1@hiroshima-u.ac.jp

Y. Harada
Division of Radiation Information Registry, Research Institute for Radiation Biology and Medicine, Hiroshima University, Hiroshima, Japan

N. Sasaki
Clinical Pathology, Kure Kyosai Hospital, Kure, Japan

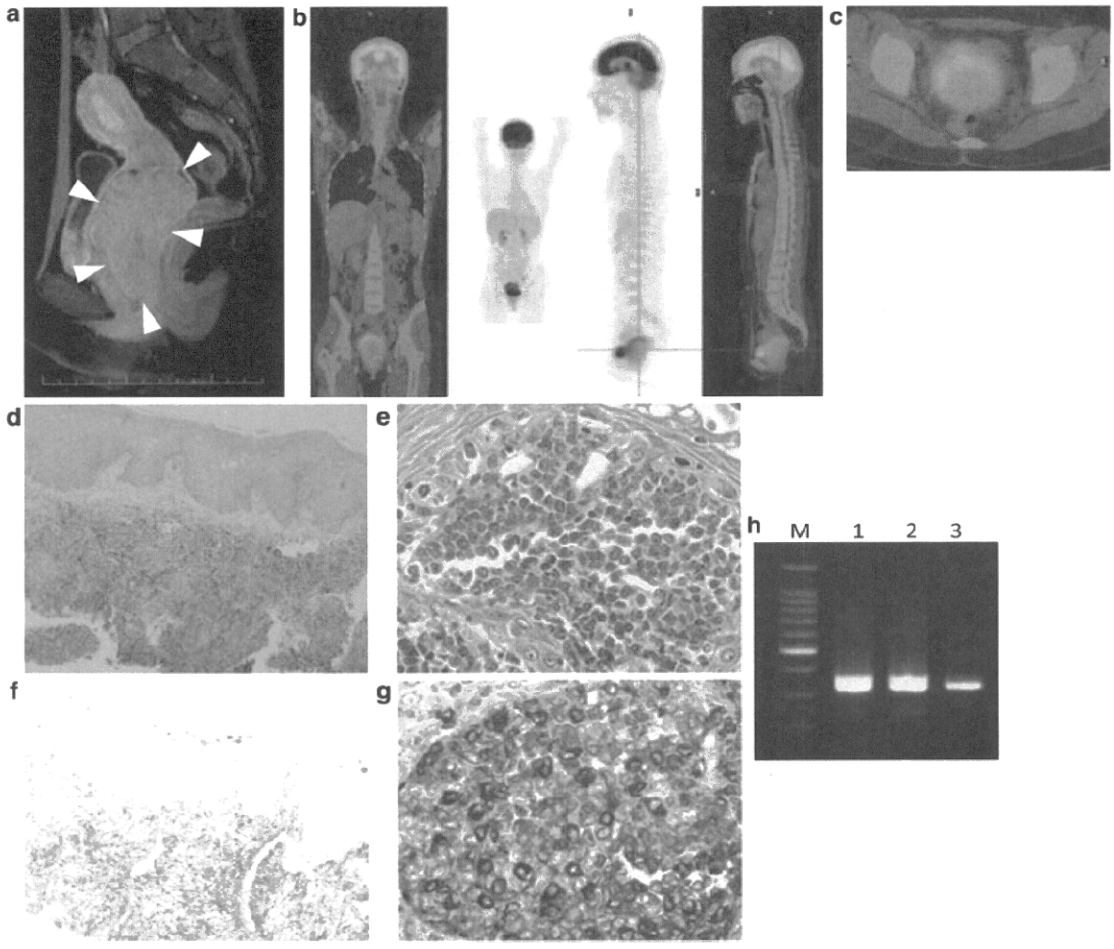

Fig. 1 Image analysis and examination of the biopsy specimen of the vaginal tumor. **a** T1 weighted MRI of the patient's pelvis at diagnosis. A large solitary tumor (indicated by *arrow heads*) is observed in the vagina. No involvement of the uterus, ovary, bladder or rectum was shown. FDG-PET/CT image of the patient's whole body (**b**) and pelvis (**c**). Brain and bladder showed high physiological uptakes. The vaginal tumor showed an increased FDG uptake, while no other region showed pathological FDG uptake. **d–g** Histology of the biopsy specimen. HE staining ×40 (**d**), ×200 (**e**) shows diffuse subepithelial infiltrate of medium sized cells with prominent nucleoli, eosinophilic granular cytoplasm and high nuclear/cytoplasmic ratio. **f** Immunohistochemical staining of the same specimen showed positive CD56 (×40). **g** Additional immunohistochemical analysis of the vaginal tumor showed positive lysozyme (×200). **h** RT-PCR analysis of the *AML1-ETO* fusion gene was positive in both the bone marrow cells and the vaginal tumor. *M* size marker (100-bp ladder), *lane 1* Kasumi-1 cell line (positive control), *lane 2* bone marrow cells from the patient, and *lane 3* vaginal tumor cells from the patient

occurs characteristically adjacent to cranial, facial, and spinal bones, and these tumors rarely appear as bulky masses [4, 5]. In t(8;21) AML associated with extramedullary manifestations, CD56 expression is frequently seen [4, 5]. CD56 is the neural cell adhesion molecule (NCAM) which mediates cell–cell and cell–substratum recognition and adhesion. The cell adhesion molecules may determine specific sites involving in malignant diseases. This can explain the high frequency of extramedullary tumor formation.

The diagnosis of GS is difficult, especially in a case without a preceding AML, because GS may be unsuspected clinically. Furthermore, it is difficult to distinguish from other hematological tumors histologically, and myeloid blasts often express aberrant lymphoid antigens, with non-Hodgkin lymphoma being the most common misdiagnosis [6]. Missing the diagnosis may lead to inappropriate therapy and increased side effects in the patient [1]. It is generally accepted that local radiotherapy is indispensable in the treatment of an early-stage NK-cell lymphoma [7]. Therefore, it is highly probable that we would have treated the unmarried young female with vaginal irradiation if the diagnosis had not been revised. As a consequence, the patient might have suffered a harmful influence on her sex life and fertility. To avoid serious diagnostic errors, active suspicion of GS and careful evaluation of myeloid morphological features are required when a less differentiated

neoplasm is encountered. Myeloperoxidase, chloroacetate esterase and lysozyme are highly sensitive and specific for GS [1, 2, 6, 8]. Moreover, bone marrow aspiration provides a valuable opportunity to find GS even if the peripheral blood count is normal. Recently, FDG-PET/CT has been reported to be a powerful tool in the diagnosis of GS [9, 10]. Changes in FDG uptake after therapy correlated with clinical outcome; the patients with negative FDG after chemotherapy continued to be disease free, whereas the disease progressed rapidly in the patients with positive FDG [9]. Therefore, FDG-PET/CT appears to be a useful tool for diagnosis and monitoring in the management of patients with GS.

In conclusion, we reported a case of giant vaginal GS that was unique with respect to both its location and symptomatology. The diagnosis of GS is often challenging, and a misdiagnosis is directly connected to inappropriate therapy and serious adverse effects. In order to prevent a misdiagnosis, the possibility of GS must be taken into consideration when encountering a morphologically immature tumor. Immunohistochemistry for detection of myeloid antigens provides useful clues for the diagnosis of GS. In addition, FDG-PET/CT may be promising tools to estimate the therapeutic effectiveness and further prognosis.

References

1. Neiman RS, Barcos M, Berard C, Bonner H, Mann R, Rydell RE, et al. Granulocytic sarcoma: a clinicopathologic study of 61 biopsied cases. Cancer. 1981;48:1426–37.
2. Garcia MG, Deavers MT, Knoblock RJ, Chen W, Tsimberidou AM, Manning JT Jr, et al. Myeloid sarcoma involving the gynecologic tract: a report of 11 cases and review of the literature. Am J Clin Pathol. 2006;125:783–90.
3. Henes M, Nauth A, Staebler A, Becker S, Henes JC. Postmenopausal bleeding as first sign of an acute myelogenous leukaemia: a case report and review of the literature. Med Oncol. 2009;27:815–9.
4. Tallman MS, Hakimian D, Shaw JM, Lissner GS, Russell EJ, Variakojis D. Granulocytic sarcoma is associated with the 8;21 translocation in acute myeloid leukemia. J Clin Oncol. 1993;11:690–7.
5. Byrd JC, Weiss RB, Arthur DC, Lawrence D, Baer MR, Davey F, et al. Extramedullary leukemia adversely affects hematologic complete remission rate and overall survival in patients with t(8;21)(q22;q22): results from Cancer and Leukemia Group B 8461. J Clin Oncol. 1997;15:466–75.
6. Menasce LP, Banerjee SS, Beckett E, Harris M. Extra-medullary myeloid tumour (granulocytic sarcoma) is often misdiagnosed: a study of 26 cases. Histopathology. 1999;34:391–8.
7. Kohrt H, Advani R. Extranodal natural killer/T-cell lymphoma: current concepts in biology and treatment. Leuk Lymphoma. 2009;50:1773–84.
8. Traweek ST, Arber DA, Rappaport H, Brynes RK. Extramedullary myeloid cell tumors. An immunohistochemical and morphologic study of 28 cases. Am J Surg Pathol. 1993;17:1011–9.
9. Aschoff P, Hantschel M, Oksuz M, Werner M, Lichy M, Vogel W, et al. Integrated FDG-PET/CT for detection, therapy monitoring and follow-up of granulocytic sarcoma. Nuklearmedizin. 2009;48:185–91.
10. Ueda K, Ichikawa M, Takahashi M, Momose T, Ohtomo K, Kurokawa M. FDG-PET is effective in the detection of granulocytic sarcoma in patients with myeloid malignancy. Leuk Res. 2010;34:1239–41.

Brief report

Clinical and genetic features of therapy-related myeloid neoplasms after chemotherapy for acute promyelocytic leukemia

Jun Imagawa,[1] Yuka Harada,[2] Takeshi Shimomura,[3] Hideo Tanaka,[4] Yoshiko Okikawa,[5] Hideo Hyodo,[1] Akiro Kimura,[1] and Hironori Harada[1]

[1]Department of Hematology and Oncology and [2]Division of Radiation Information Registry, Research Institute for Radiation Biology and Medicine, Hiroshima University, Hiroshima, Japan; [3]National Hospital Organization Hiroshima-Nishi Medical Center, Ohtake, Japan; [4]Hiroshima City Asa Hospital, Hiroshima, Japan; and [5]National Hospital Organization Kure Medical Center, Kure, Japan

Acute promyelocytic leukemia (APL) is a highly curable disease with excellent complete remission and long-term survival rates. However, the development of therapy-related myeloid neoplasms (t-MN) is being reported with increasing frequency in patients successfully treated for APL. We attempted to clarify the different clinical features and hematologic findings between t-MN and relapse cases, and to identify gene alterations involved in t-MN. We compared 10 relapse and 11 t-MN cases that developed in 108 patients during their first complete remission from APL. At APL diagnosis, t-MN patients had lower white blood cell counts than did relapse patients ($P = .048$). Overall survival starting from chemotherapy was significantly worse in t-MN patients than in relapse patients ($P = .022$). The t-MN cases were characterized as CD34$^+$/HLA-DR$^+$ and *PML-RARA*$^-$, and 4 *RUNX1/AML1* mutations were detected. T-MN is easily distinguished from APL relapse by evaluating these hematologic features, and it may originate from primitive myeloid cells by chemotherapy-induced *RUNX1* mutations. (*Blood*. 2010;116(26):6018-6022)

Introduction

Acute promyelocytic leukemia (APL) is a distinct subtype of acute myeloid leukemia (AML) characterized by a t(15;17) translocation leading to a *PML-RARA* fusion gene. APL is a highly curable disease with excellent complete remission (CR) and long-term survival rates. All-*trans* retinoic acid (ATRA) combined with anthracycline-based chemotherapy yields a CR rate of approximately 90% for newly diagnosed APLs. The relapse rate is approximately 20%, and with the development of new molecular target therapies such as arsenic trioxide, a cure can now be expected even for relapsed patients.

However, the development of therapy-related myeloid neoplasms (t-MN) is being reported with an increasing frequency of 0.97% to 6.5% in patients successfully treated for APL.[1-3] Patients are typically in hematologic and cytogenetic remission for APL, and at follow-up after treatment, hematologic abnormalities may be detected without evidence of the original *PML-RARA* fusion gene seen at APL diagnosis. The t-MN secondary to APL is usually difficult to treat, and it is one of the prognosis-limiting factors for the curable APL disease. Therefore, we attempted to clarify the different clinical features and hematologic findings between t-MN and relapsed APL cases, and to identify gene alterations associated with t-MN.

Methods

Patients

Patients with APL were diagnosed at Hiroshima University Hospital and its affiliated hospitals between 1996 and 2008. Diagnoses of APL were initially made morphologically according to the French-American-British classification and were confirmed by the presence of t(15;17) and/or presence of the *PML/RARA*. Patients were treated with ATRA combined with chemotherapy and with intensified maintenance chemotherapy.[4,5] Patients who were resistant to ATRA therapy were treated with arsenic trioxide. Drugs used during APL treatment were idarubicin, cytarabine, mitoxantrone, daunorubicin, etoposide (VP-16), behenoyl cytarabine, mercaptopurine, vindesine, and aclarubicin. All patients received an intrathecal administration of methotrexate, cytarabine, and prednisolone during consolidation therapy. Patients with APL were examined as approved by the Institutional Review Board at Hiroshima University. Patients gave written informed consent in accordance with the Declaration of Helsinki.

Identification of *RUNX1*, *CEBPA*, *FLT3*, and *NRAS* mutations

Mononuclear cells were isolated from bone marrow samples, and genomic DNA and total RNA were prepared as described previously.[6] Identification of *RUNX1*, *CEBPA*, *FLT3*, and *NRAS* mutations was performed as described previously.[6-8]

Statistical analysis

Probabilities of survival were estimated using the Kaplan-Meier method and compared by the log-rank test.

Results and discussion

A total of 124 patients with APL were newly diagnosed and were consecutively enrolled in the study. The median age at diagnosis was 52 years (range, 18-86 years). An 86-year-old patient died of

Submitted June 9, 2010; accepted September 15, 2010. Prepublished online as *Blood* First Edition paper, September 22, 2010; DOI 10.1182/blood-2010-06-289389.

The publication costs of this article were defrayed in part by page charge payment. Therefore, and solely to indicate this fact, this article is hereby marked "advertisement" in accordance with 18 USC section 1734.

Table 1. Treatments for primary APL and for t-MN

	At APL				At t-MN	
Disease type/patient no.	Protocol*	VP-16 in consolidation therapy, mg/m²†	VP-16 in maintenance therapy, mg/m²‡	Presence of myelodysplastic phase	Therapy	Outcome
t-MN with progression to AML						
10	APL92	500	480	+	Intensive chemotherapy	Died of disease progression
18	APL97	500	480	+	Intensive chemotherapy	Died of disease progression
19	APL97	500	480	+	Intensive chemotherapy	Died of disease progression
22	APL97	500	480	−	Intensive chemotherapy	Died of disease progression
48	APL97	500	480	+	Intensive chemotherapy	Alive in CR
79	APL97	500	480	+	Intensive chemotherapy	Died of disease progression
83	APL97	500	480	+	Intensive chemotherapy	Died of disease progression
108	APL97	500	0	+	Intensive chemotherapy then allogeneic stem cell transplantation	Died of disease progression
109	APL97	500	0	+	Intensive chemotherapy	Died of disease progression
t-MN without progression to AML (t-MDS-RCMD)						
7	APL92	500	480	+	Supportive care	Alive without progression
49	APL97	500	480	+	Supportive care	Alive without progression

*Two consecutive protocols (APL92[4] or APL97[5] of the Japan Adult Leukemia Study Group) were used.
†A total of 100 mg/m² for 5 days.
‡A total of 80 mg/m² on days 1, 3, and 5 in the second and the sixth course.

lung hemorrhage before starting induction therapy. Other patients received induction therapy, including ATRA with chemotherapy. Two patients were resistant to ATRA therapy and were treated with arsenic trioxide. Six patients who were 70 years of age or older died during induction therapy, whereas 117 patients (94.4%) achieved CR. After achieving CR, 2 patients dropped out of the study because they moved to a distant place, and 2 patients could not continue the therapy because of neuropsychologic diseases and died within 1 year. Others received intensive consolidation chemotherapy, but 5 patients died of therapy-related complications. All of the remaining 108 patients completed consolidation therapy. The predicted 10-year overall survival was 74.6% for the whole population, and 81.4% and 36.9% in patients younger than 70 years and 70 years or older, respectively. Thus, the efficacy of the treatment for APL patients in this study is comparable with that reported in clinical trials.[4,5]

After a median follow-up of 8.6 years (range, 1.7-16.3 years), 5 patients died of nonhematologic causes, 10 patients (9.3%) relapsed, and 11 patients (10.2%) developed t-MN among the 108 patients during their first CR from APL. We also analyzed 61 patients with *RUNX1-ETO* or *CBFB-MYH11* (core-binding factor leukemia) during the same research period and found 13 relapses (21.3%) but no t-MN. Thus, there is a possibility that t-MN after successful treatment of APL may be more popular than AML other than APL. We noted more t-MN patients instead of fewer relapse patients compared with other reports. The fact that all patients in this study had received VP-16 for consolidation therapy whereas no VP-16 was administered in other trials could explain, in part, the higher incidence of t-MN.[3] Furthermore, the accumulation of chemotherapeutic agents in the maintenance phase may increase the risk of t-MN.[5] Meanwhile, there is a possibility that t-MN might have been diagnosed as relapsing APL because of positive *PML-RARA* from coexisting APL cells. Therefore, we attempted to clarify the differences in clinical features and hematologic findings between t-MN and relapsed APL patients after successful treatment of APL.

The patients who developed t-MN with progression to AML, therapy-related myelodysplastic syndrome, refractory cytopenia with multilineage dysplasia (t-MDS-RCMD), or relapse are shown in Tables 1 and 2. The median white blood cell (WBC) count at APL diagnosis was 6940/μL (range, 1.1-42.6/μL) in the t-MN patients and 33 630/μL (range, 1.1-148.6/μL) in the relapse patients, whereas it was 13 130/μL (range, 0.3-152.8/μL) in the disease-free patients who remained continuously in their first CR for 1.5 to 16.1 years (median, 8.3 years). The WBC count was significantly lower in the t-MN patients than in the relapse patients ($P = .048$). Relapse risk based on pretreatment WBC count and platelet count indicated that most of the t-MN patients were distributed in low- and intermediate-risk groups (Figure 1A). In particular, the WBC count at APL diagnosis was less than or equal to 4500/μL in most of the t-MN patients, whereas it was more than 4500/μL in the relapse patients. Previous reports also showed that most of the t-MN patients had a low WBC count.[3,9] After the first APL diagnosis, the median intervals were 2.6 years (range, 0.6-10.1 years) to relapse, 2.3 years (range, 1.6-3.0 years) to t-MDS-RCMD, and 3.3 years (range, 1.0-9.7 years) to t-MN with progression to AML ($P = .83$). However, overall survival from the start of chemotherapy was significantly worse for the t-MN with progression to AML patients than for the relapse patients ($P = .022$, Figure 1B). VP-16 or intensive maintenance chemotherapy may reduce the risk of relapse; however, the frequency of t-MN may increase. Recent therapeutic approaches in the treatment of refractory APL may improve the second CR rate. Our results suggest that preventing t-MN may be more important than preventing relapse, especially in patients with low WBCs.

We examined surface markers of the leukemic cells (Figure 1C). At the primary APL diagnosis, most of the leukemic cells from the APL patients showed $CD34^-HLA\text{-}DR^-CD33^+$ phenotypes. At relapse, the phenotypes showed the same pattern, whereas at the t-MN CD34 and HLA-DR phenotypes changed to positive and the positivity of CD33 became lower. The relapse patients and the t-MN patients were easily distinguished by their CD34/HLA-DR distribution pattern; APL cells were $CD34^-HLA\text{-}DR^-$, whereas t-MN cells were $CD34^+$ and/or $HLA\text{-}DR^+$ (Figure 1D). These results indicate that the leukemic cells changed to primitive myeloid cells when t-MN developed after successful treatment of APL, and they were considered to have an independent clonal origin.[10]

Table 2. Clinical features and genetic findings for the patients with t-MN and relapsed APL

	At APL diagnosis (A)							Interval from A to B, y	At relapse or t-MN (B)					Survival from B, y
Disease type/ patient no.	Age, y/sex	WBCs, $\times 10^9$/L	Platelets, $\times 10^9$/L	FAB classification	Karyotype*	*PML-RARA*	Class I mutations†		FAB classification	Karyotype*	*PML-RARA*	Other class II abnormalities†	Class I mutations†	
t-MN with progression to AML														
10‡	38/F	1.10	17	M3	46,XX[20]	+	−	5.1	RAEBt	45,XX,-7[19]/46,idem,+21[1]	−	*RUNX1* D171N	*NRAS* G12V	0.8
18	38/M	1.10	43	M3	46,XY,t(15;17)(q22;q21)[17]/ 46,XY[3]	+	−	4.0	RAEB	45,XY,-7[3]/46,XY[17]	−	*RUNX1* D171G	−	2.0
19	35/M	42.60	10	M3	46,XY,t(15;17)(q22;q21)[20]	+	−	2.4	RAEBt	46,XY,t(7;15)(q11;q11),der(12)t(12;17)(p11;q21), t(16;21)(q24;q22), add(17)(q11),add(19)(p13), del(21)(q21)[3]/46,idem, der(18)t(15;18)(q11;p11) [6]/ 46,XY[11]	−	*RUNX1-MTG16*	−	1.9
22	48/M	1.80	110	M3	46,XY,t(15;17)(q22;q21)[18]/ 46,XY[2]	+	−	9.7	M0	46,XY,add(13)(q32)[19]/46,XY[1]	−	−	−	0.8
48	57/F	4.10	16	M3	46,XX,t(15;17)(q22;q21)[19]/ 46,XX[1]	+	−	1.4	M1	46,XX,t(6;11)(q21;q23)[16]/46,XX[4]	−	*MLL-FOXO3*	−	> 8.7
79	62/M	2.20	54	M3	46,XY,t(15;17)(q22;q21)[19]/ 46,XY[1]	+	−	2.6	RAEB	46,XY,add(2)(p23),inv(5)(p11q13), add(11)(q23)[14]/46,idem, inv(2)(p23q11)[4]/47,idem,+13[2]	−	*RUNX1* S295fsX571	−	1.3
83	42/M	1.20	144	M3	46,XY,t(15;17)(q22;q21)[17]/ 46,XY[3]	+	−	2.5	RAEB	45,XY,-7[19]/46,XY[1]	−	*RUNX1* G172W	−	1.7
108	18/M	14.40	36	M3	46,XY,t(15;17)(q22;q21)[20]	+	−	1.0	M4	46,XY,t(11;16)(q23;p13.3)[6] / 46,XY[14]	−	*MLL-CBP*	*FLT3*ITD	2.6
109	65/M	1.68	41	M3	46,XY,t(15;17)(q22;q21)[20]	+	−	1.3	RAEB	46,XY[20]	−	*CEBPA* Q305P	−	1.7
t-MN without progression to AML (t-MDS-RCMD)														
7	54/F	4.50	6	M3	46,XX,t(15;17)(q22;q21)[20]	+	−	1.6	RA	46,XX,del(20)(q11)[15]/46,XX[5]	−	−	−	> 13.4
49	67/M	1.62	42	M3	45,X,-Y,t(15;17)(q22;q21), del(14)(q13q22)[18]/ 46,XY[2]	+	−	3.0	RA	46,XY,del(20)(q1?)[3]/46,XY[17]	−	−	−	> 6.9
Relapse														
8	54/M	1.30	258	M3	46,XY,t(15;17)(q22;q31)[20]	+	−	3.4	M3	46,XY,add(9)(q22),add(13)(p11), t(15;17)(q22;q21)[3]/46,XY[17]	+	−	−	> 11.4
12	32/M	12.67	7	M3	46,XY,t(9;X)(p24;q22), t(15;17)(q22;q21)[20]	+	−	0.6	M3	ND	+	−	*FLT3*ITD	2.4§
13	38/M	95.70	35	M3	47,XY,+mar1[17]/46,XY[3]	+	−	10.1	M3	48,XY,+mar1x2[13]/46,XY[7]	+	−	−	> 3.6
17	53/F	4.80	52	M3	46,XX[20]	+	−	2.0	M3	46,XX[20]	+	−	−	> 11.1
25	58/F	148.60	31	M3v	46,XX[20]	+	*FLT3*ITD	1.5	M3v	46,XX[20]	+	−	*FLT3*ITD	0.8
38	64/F	15.70	27	M3	46,XX,t(15;17)(q22;q21)[20]	+	*FLT3*ITD	1.0	M3	46,XX,t(15;17)(q22;q21)[20]	+	−	*FLT3*ITD	1.7
78	39/M	7.03	13	M3	48,XY,+8,+8,t(15;17)(q22;q21)[10]/49,idem,+21[9]/46,XY[1]	+	−	1.1	M3	ND	+	−	−	0.9‖
85	19/M	1.10	152	M3v	49,XY,t(15;17)(q22;q21),+mar1, +mar2, +mar3[16]/46,XY[4]	+	−	2.5	M3v	49,XY,t(15;17)(q22;q21),+mar1, +mar2, +mar3[15]/46,XY[5]	+	−	−	> 4.2
88	46/M	4.60	47	M3	46,XY[20]	+	*FLT3*ITD	1.8	M3	46,XY[20]	+	−	*FLT3*ITD	> 4.8
95	55/M	44.80	21	M3v	46,XY,t(15;17)(q22;q31)[20]	+	−	1.8	M3v	46,XY,t(15;17)(q22;q21)[17] / 46,XY[3]	+	−	−	> 4.0

M3v indicates M3 variant; ND, not done; +, positive; and −, negative.

*Numbers in square brackets are cell numbers.

†Class I mutations include the *FLT3* and *NRAS* mutations, and other class II abnormalities include the chimeric proteins and the *RUNX1* and *CEBPA* mutations.

‡This patient was reported previously[6] (case 8).

§This patient died from an accident during the third CR.

‖This patient refused reinduction therapy and died of cerebral bleeding.

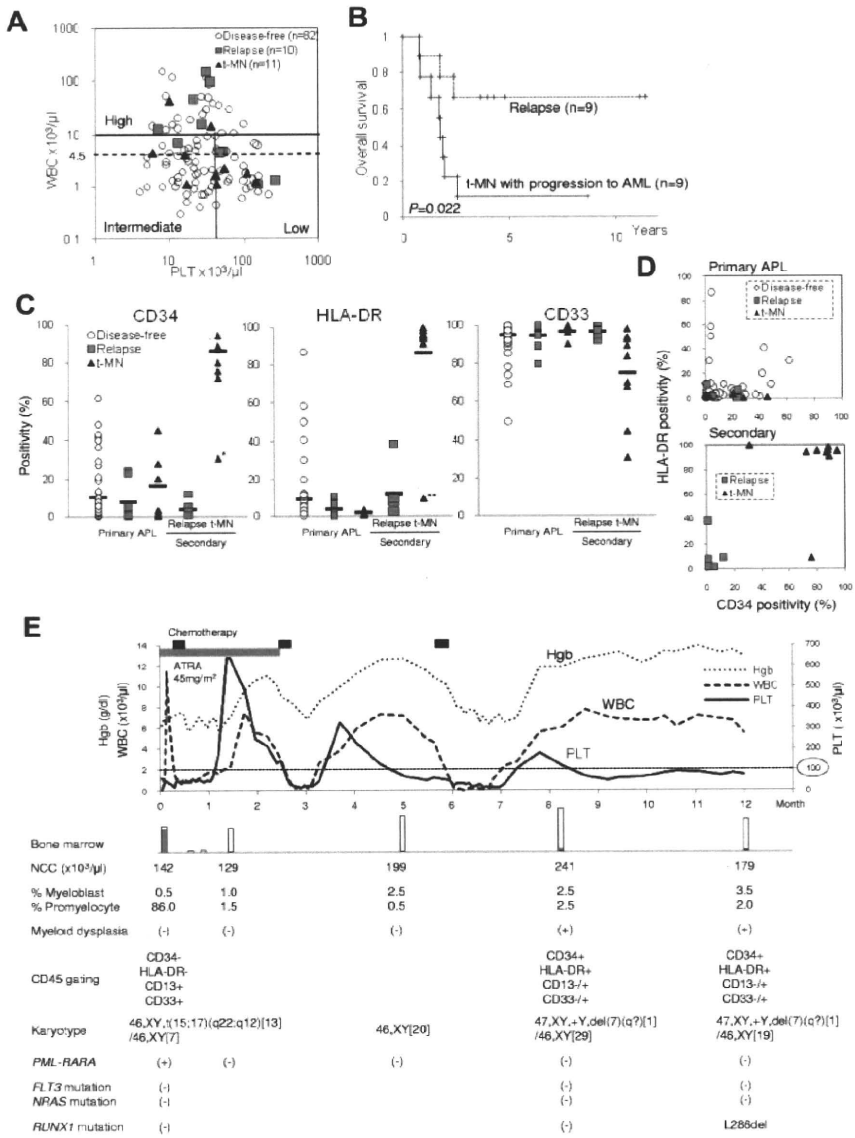

Figure 1. T-MN is easily distinguished from APL relapse by evaluating hematologic features. (A) Relapse risk was predicted by pretreatment WBC and platelet counts of each patient at APL diagnosis. Patients with APL could be stratified into low-risk (WBC count $\leq 10 \times 10^3/\mu L$, platelet count $> 40 \times 10^3/\mu L$), intermediate-risk (WBC count $\leq 10 \times 10^3/\mu L$, platelet count $\leq 40 \times 10^3/\mu L$), and high-risk (WBC count $> 10 \times 10^3/\mu L$) groups. The number of patients in high-, intermediate-, and low-risk groups were 21 (25.6%), 40 (48.8%), and 21 (25.6%), respectively, in the disease-free population, whereas they were 5 (50%), 1 (10%), and 4 (40%), respectively, in the relapse patients and 2 (18.2%), 3 (27.3%), and 6 (54.5%), respectively, in the t-MN patients. (B) Overall survival from date of starting chemotherapy for the relapsed APL or t-MN patients after successful APL treatment. Patients with t-MDS-RCMD and patient 78 who were treated without chemotherapy were excluded. (C) Surface-marker analysis of the leukemic cells by the CD45RO gating method. Because of their low blast percentages, t-MDS-RCMD patients were excluded. *Patient 48 and **patient 109 were mixed lineage leukemia with *MLL* chimera. (D) APL relapse and t-MN were distinguished by CD34/HLA-DR expression patterns. (E) Clinical course of a 69-year-old man. The patient developed APL in 2009, although he had a normal blood count until 2008. Eight months after starting the treatment for APL with ATRA and chemotherapy, the patient showed persistent thrombocytopenia and trilineage dysplasia (megaloblastic changes of erythroblasts, decreased granules of granulocytes, and micromegakaryocytes), and he was diagnosed as t-MN.

To confirm their clonality, gene abnormalities that may play an important role in leukemogenesis were analyzed.[11] All of the relapse patients had the *PML-RARA* gene, whereas none of the patients with t-MN had *PML-RARA*. Instead, we found translocations involving 21q22 of *RUNX1* (*RUNX1-MTG16*) or 11q23 of *MLL* (*MLL-FOXO3* and *MLL-CBP*; Table 2), as previously reported.[9,12,13] Both of the t-MDS-RCMD patients had an isolated del(20q), which may be associated with a good prognosis. Furthermore, 4 *RUNX1* mutations and one *CEBPA* mutation were detected. These abnormalities were not detected at the primary APL diagnosis or in the relapsed patients with APL or core-binding factor leukemia. *RUNX1* mutations are known to be frequently involved in t-MN; however, no such reports included t-MN from APL. One patient with a *RUNX1* mutation also acquired an *NRAS* mutation at t-MN. Three of 4 *RUNX1* mutations were associated with monosomy 7, which is frequently reported in t-MN after successful treatment of APL.[3,9] It is possible that previously reported monosomy 7 cases were also associated with *RUNX1* mutations, but this was not investigated in the earlier studies.

In addition, a recent case of t-MN at 8 months after APL diagnosis showed a phenotype of increasing $CD34^+HLA\text{-}DR^+$ cells, gating on the CD45RO (Figure 1E). Karyotypic analysis showed a del(7q) abnormality, although the percentage of blasts was less than 5% in the bone marrow, and the *RUNX1* mutation was detected at 12 months. Monitoring of surface markers, karyotype, and the *RUNX1* mutation, as

well as *PML-RARA* monitoring, may be useful for the early diagnosis of t-MN in patients successfully treated for APL.

A previous report showed that *RUNX1* mutations may have a leukemogenic potential in $CD34^+$ cells from patients in the chronic phase of myeloproliferative neoplasms.[7] In addition, in APL, it is assumed that *RUNX1* or other abnormalities may be induced in $CD34^+$ cells during chemotherapy resulting in t-MN after successful treatment of APL. Some patients with *JAK2*$V617F^+$ myeloproliferative neoplasms were reported to transform to *JAK2*$V617F^-$ AML, suggesting that leukemia developed from a pre-*JAK2* hematopoietic stem cell[14] or from a normal hematopoietic stem cell.[15] *PML-RARA*$^-$ t-MN may also develop from a "receptive" hematopoietic stem cell or from a normal hematopoietic stem cell, which is a myeloid committed progenitor, by the accumulation of chemotherapy-induced gene abnormalities, including *RUNX1* mutations.

Acknowledgments

The authors thank Ryoko Matsumoto-Yamaguchi, who provided excellent technical support in carrying out these experiments.

This work was supported in part by the Ministry of Education, Culture, Sports, Science and Technology of Japan (Grants-in-Aid for Scientific Research: grants 21591206 and 22591038, H. Harada, Y.H.). This work was carried out in part at the Analysis Center of Life Science, Hiroshima University.

Authorship

Contribution: J.I. collected data and wrote the paper; Y.H. assembled and analyzed the data and revised the manuscript; T.S., H.T., Y.O., H. Hyodo, and A.K. provided patient samples and clinical information; and H. Harada designed the research and revised the manuscript.

Conflict-of-interest disclosure: The authors declare no competing financial interests.

Correspondence: Hironori Harada, Department of Hematology and Oncology, Research Institute for Radiation Biology and Medicine, Hiroshima University, 1-2-3 Kasumi, Minami-ku, Hiroshima 734-8553, Japan; e-mail: herf1@hiroshima-u.ac.jp.

References

1. Latagliata R, Petti MC, Fenu S, et al. Therapy-related myelodysplastic syndrome-acute myelogenous leukemia in patients treated for acute promyelocytic leukemia: an emerging problem. *Blood.* 2002;99(3):822-824.
2. Garcia-Manero G, Kantarjian HM, Kornblau S, Estey E. Therapy-related myelodysplastic syndrome or acute myelogenous leukemia in patients with acute promyelocytic leukemia (APL). *Leukemia.* 2002;16(9):1888.
3. Lobe I, Rigal-Huguet F, Vekhoff A, et al. Myelodysplastic syndrome after acute promyelocytic leukemia: the European APL group experience. *Leukemia.* 2003;17(8):1600-1604.
4. Asou N, Adachi K, Tamura U, et al. Analysis of prognostic factors in newly diagnosed patients with acute promyelocytic leukemia: the APL92 study of the Japan Adult Leukemia Study Group (JALSG). *Cancer Chemother Pharmacol.* 2001; 48(suppl 1):S65-S71.
5. Asou N, Kishimoto Y, Kiyoi H, et al. A randomized study with or without intensified maintenance chemotherapy in patients with acute promyelocytic leukemia who have become negative for PML-RARalpha transcript after consolidation therapy: the Japan Adult Leukemia Study Group (JALSG) APL97 study. *Blood.* 2007;110(1):59-66.
6. Harada H, Harada Y, Niimi H, Kyo T, Kimura A, Inaba T. High incidence of somatic mutations in the AML1/RUNX1 gene in myelodysplastic syndrome and low blast percentage myeloid leukemia with myelodysplasia. *Blood.* 2004;103(6): 2316-2324.
7. Ding Y, Harada Y, Imagawa J, Kimura A, Harada H. AML1/RUNX1 point mutation possibly promotes leukemic transformation in myeloproliferative neoplasms. *Blood.* 2009;114(25):5201-5205.
8. Niimi H, Harada H, Harada Y, et al. Hyperactivation of the RAS signaling pathway in myelodysplastic syndrome with AML1/RUNX1 point mutations. *Leukemia.* 2006;20(4):635-644.
9. Zompi S, Viguie F. Therapy-related acute myeloid leukemia and myelodysplasia after successful treatment of acute promyelocytic leukemia. *Leuk Lymphoma.* 2002;43(2):275-280.
10. Andersen MK, Pedersen-Bjergaard J. Therapy-related MDS and AML in acute promyelocytic leukemia. *Blood.* 2002;100(5):1928-1929; author reply 1929.
11. Gilliland DG. Hematologic malignancies. *Curr Opin Hematol.* 2001;8(4):189-191.
12. Snijder S, Mellink CH, van der Lelie H. Translocation (2;11)(q37;q23) in therapy-related myelodysplastic syndrome after treatment for acute promyelocytic leukemia. *Cancer Genet Cytogenet.* 2008;180(2):149-152.
13. Park TS, Choi JR, Yoon SH, et al. Acute promyelocytic leukemia relapsing as secondary acute myelogenous leukemia with translocation t(3; 21)(q26;q22) and RUNX1-MDS1-EVI1 fusion transcript. *Cancer Genet Cytogenet.* 2008;187(2): 61-73.
14. Levine RL, Gilliland DG. Myeloproliferative disorders. *Blood.* 2008;112(6):2190-2198.
15. Beer PA, Delhommeau F, LeCouedic JP, et al. Two routes to leukemic transformation after a JAK2 mutation-positive myeloproliferative neoplasm. *Blood.* 2010;115(14):2891-2900.

Two types of C/EBPα mutations play distinct but collaborative roles in leukemogenesis: lessons from clinical data and BMT models

Naoko Kato,[1,2] Jiro Kitaura,[1] Noriko Doki,[1] Yukiko Komeno,[1] Naoko Watanabe-Okochi,[3] Katsuhiro Togami,[1] Fumio Nakahara,[1,2] Toshihiko Oki,[1,2] Yutaka Enomoto,[1] Yumi Fukuchi,[4] Hideaki Nakajima,[4] Yuka Harada,[5] Hironori Harada,[6] and Toshio Kitamura[1,2]

Divisions of [1]Cellular Therapy and [2]Stem Cell Signaling, Institute of Medical Science, University of Tokyo, Tokyo, Japan; [3]Department of Hematology and Oncology, Graduate School of Medicine, University of Tokyo, Tokyo, Japan; [4]Division of Hematology, Department of Internal Medicine, Keio University School of Medicine, Tokyo, Japan; [5]International Radiation Information Center, Research Institute for Radiation Biology and Medicine, Hiroshima University, Hiroshima, Japan; and [6]Department of Hematology and Oncology, Research Institute for Radiation Biology and Medicine, Hiroshima University, Hiroshima, Japan

Two types of mutations of a transcription factor CCAAT-enhancer binding protein α (C/EBPα) are found in leukemic cells of 5%-14% of acute myeloid leukemia (AML) patients: N-terminal mutations expressing dominant negative p30 and C-terminal mutations in the basic leucine zipper domain. Our results showed that a mutation of C/EBPα in one allele was observed in AML after myelodysplastic syndrome, while the 2 alleles are mutated in de novo AML. Unlike an N-terminal frame-shift mutant (C/EBPα-N^m)–transduced cells, a C-terminal mutant (C/EBPα-C^m)–transduced cells alone induced AML with leukopenia in mice 4-12 months after bone marrow transplantation. Coexpression of both mutants induced AML with marked leukocytosis with shorter latencies. Interestingly, C/EBPα-C^m collaborated with an Flt3-activating mutant Flt3-ITD in inducing AML. Moreover, C/EBPα-C^m strongly blocked myeloid differentiation of 32Dcl3 cells, suggesting its class II mutation-like role in leukemogenesis. Although C/EBPα-C^m failed to inhibit transcriptional activity of wild-type C/EBPα, it suppressed the synergistic effect between C/EBPα and PU.1. On the other hand, C/EBPα-N^m inhibited C/EBPα activation in the absence of PU.1, despite low expression levels of p30 protein generated by C/EBPα-N^m. Thus, 2 types of C/EBPα mutations are implicated in leukemogenesis, involving different and cooperating molecular mechanisms. (*Blood*. 2011; 117(1):221-233)

Introduction

The CCATT/enhancer binding protein α (C/EBPα) transcription factor is a critical regulator of proliferation and differentiation in myeloid cells.[1,2] C/EBPα consists of an N-terminal transcriptional activation domain and a C-terminal basic leucine zipper (bZIP) domain.[3-5] Two isoforms of C/EBPα proteins are generated from different translation start sites: a full-length 42-kDa protein (p42) and a truncated 30-kDa protein (p30) that lacks an N-terminal transcriptional activation domain. C/EBPα-p30 isoform inhibits C/EBPα-p42–mediated transcription.[6-8] Importantly, C/EBPα promotes differentiation both by up-regulation of lineage-specific gene products[9-11] and by proliferation arrest.[12] Recent studies have indicated that C/EBPα-induced growth arrest is regulated by its interaction with other molecules involved in growth control: E2F,[13-15] Max,[16] and SWI/SNF chromatin remodeling complexes.[17] For example, repression of E2F activity by E2F-C/EBPα interaction results in the down-regulation of c-Myc, leading to granulocytic differentiation.[18,19]

According to several studies, *CEBPA* mutations are found in 5%-14% of acute myeloid leukemia (AML) patients belonging to the French-American-British subtypes M1, M2, or in some cases M4.[8,20-22] The mutations of the *CEBPA* gene can be largely categorized into 2 types: one is an N-terminal frame-shift mutation disrupting p42 and producing p30 as a major product, and the other is a C-terminal in-frame mutation disrupting the bZIP region. Interestingly, most AML patients with *CEBPA* mutations have both mutations simultaneously,[23-25] and such patients displayed a favorable outcome.[22,26] On the other hand, AML patients with single *CEBPA* mutations did not express a distinctive signature, presumably due to a variety of associating gene alterations, including Flt3 activating mutations. Related to this, involvement of single *CEBPA* mutations with myelodysplastic syndrome (MDS) remains to be clarified.[27,28]

Analysis of mice with genetic alterations in the *CEBPA* locus has contributed to delineation of molecular mechanisms by which *CEBPA* mutations induce leukemia. Conditional deficiency of C/EBPα led to a differentiation block at the transition between common myeloid progenitors and granulocyte/monocyte progenitors but not to development of leukemia.[1] However, $Cebpa^{L/L}$ mice, expressing only p30 as C/EBPα protein, developed myeloid leukemia with complete penetration.[29] On the other hand, $Cebpa^{BRM2/BRM2}$ mice, carrying a point mutation in the bZIP domain that dampened E2F interaction, showed only preleukemic features.[14] Interestingly, the same group has recently reported combinational effects of the C-terminal and the N-terminal mutations on leukemogenesis by using $Cebpa^{L/L}$ mice, $Cebpa^{K/K}$ mice carrying the K313 duplication in the C-terminal domain, and $Cebpa^{K/L}$ mice.[29,30] They proposed that efficient leukemogenesis is caused by the combination of both premalignant HSC expansion induced by

Submitted February 17, 2010; accepted September 22, 2010. Prepublished online as *Blood* First Edition paper, September 30, 2010; DOI 10.1182/blood-2010-02-270181.

The online version of this article contains a data supplement.

The publication costs of this article were defrayed in part by page charge payment. Therefore, and solely to indicate this fact, this article is hereby marked "advertisement" in accordance with 18 USC section 1734.

C-terminal *CEBPA* mutation and residual myeloid lineage commitment maintained by the N-terminal *CEBPA* mutation.[30]

Causative gene alterations in hematologic malignancies have been extensively studied, and it is now recognized that multiple mutations contribute to development of leukemia. These gene alterations are categorized into 2 groups, class I and class II mutations.[31,32] Class I mutations include activating mutations of *FLT3*, *C-KIT*, *JAK2*, *SHP2*, and *RAS*, or inactivating mutations of *TP53* and *NF-1*, and induce proliferation or block apoptosis of hemopoietic cells. On the other hand, class II mutations disrupt normal functions of transcription factors and chromosome-modifying enzymes including *MLL*, *RUNX1*, *RARA*, and *PU.1* and hamper differentiation of hemopoietic cells. Combinations of class I and class II mutations are frequently observed in patients' leukemic cells.[33,34] In addition, we and others presented evidence that class I and class II mutations collaborate in the development of leukemia in mouse models.[35,36] Among a variety of gene alterations found in leukemia, *CEBPA* mutations are unique because different *CEBPA* mutations are frequently found on different alleles in leukemic cells of de novo AML.[22-26]

In the present study, we searched for mutations of the *CEBPA* gene in patients with myeloid malignancies, and found N- and C-terminal double mutations in patients with de novo AML. In patients with MDS/AML or therapy-related AML or MDS, only N- or C-terminal single mutation was identified. We chose a C-terminal mutation 304_323dup (hereafter called C/EBPα-C^m) and an N-terminal mutation (T60fsX159) (hereafter C/EBPα-N^m) for further analysis that had been isolated as double *CEBPA* mutations in a de novo AML patient. To evaluate the effects of these mutations on leukemogenesis, we used a mouse bone marrow transplantation (BMT) model. Interestingly, unlike the phenotype in $Cebpa^{K/K}$, $Cebpa^{K/+}$, $Cebpa^{BRM2/BRM2}$, or $Cebpa^{BRM2/+}$ mice,[14,29,30] C/EBPα-C^m alone induced AML with leukopenia in transplanted mice after BMT. We also confirmed the efficient induction of AML by coexpression of C/EBPα-C^m and C/EBPα-N^m. We will discuss the possible molecular mechanisms by which C/EBPα-N^m worked in concert with C/EBPα-C^m in accelerating leukemogenesis.

Methods

Patients and samples

We chose patients with hematologic diseases (224 MDS/AML patients, 71 therapy-related AML or MDS patients, and 89 de novo AML patients, who had been diagnosed at Hiroshima University Hospital between 1985 and 2007, are not a consecutive series of patients). All studies were approved by the Institutional Review Board at Hiroshima University and the ethics committee of the University of Tokyo (approval no. 20-10-0620). Patients' informed consents were obtained in accordance with the Declaration of Helsinki. *CEBPA* mutation screening by polymerase chain reaction (PCR)–single strand conformation polymorphism analysis and identification of *CEBPA*, *AML1*, *N-RAS*, *FLT3*, *PTPN11*, *C-KIT*, and *TP53* mutations was performed as described previously.[37]

Retroviral vectors

We used 2 C/EBPα mutants, N^m or C^m, as well as C/EBPα wild-type (WT) and C/EBPα N-terminal truncated p30 (p30). C/EBPα-WT, p30, N^m, or C^m, which was tagged with a FLAG or Myc epitope at the C terminus, was inserted upstream of the internal ribosome entry site-enhanced green fluorescent protein (IRES-EGFP) cassette of pMYs-IG to generate pMYs-FLAG or Myc-tagged CEBPα-WT, p30, N^m, or C^m-IG, respectively. Similarly, these fragments were subcloned into pMXs-IRES-puro (pMXs-IP), pMXs-IRES-blasticidin (pMXs-IB), or pMYs-IRES-dsRED (pMYs-IR). Flt3-ITD cDNA, which was derived from patient's leukemic cells harboring a 20-amino acid tandem duplication called M3[38,39] was subcloned into pMYs-IG to generate pMYs-Flt3-ITD-IG. Human granulocyte colony-stimulating factor receptor (G-CSF-R) cDNA, a kind gift from Dr Shigekazu Nagata (Kyoto University, Kyoto, Japan), was subconed into pMXs-IB to generate pMXs-G-CSF-R-IB.

Retroviral infection was done as described previously.[40] Briefly, retroviruses were generated by transient transfection of Plat-E packaging cells with FuGENE 6 (Roche Diagnostics).[41,42] Growth of transduced 32Dcl3 cells, which were subject to the drug selection with 1 μg/mL puromycin or 10 μg/mL blasticidin, was estimated by quantitating luminescence as described previously.[43]

Flow cytometric analysis

Briefly, cells were stained with phycoerythrin-conjugated antibodies (Abs) or biotinylated Abs and phycoerythrin/Cy5-streptavidin (eBioscience). Flow cytometric analysis of the stained cells was performed with FACSCalibur flow (BD Biosciences) equipped with FlowJo Version 7.2.4 software (TreeStar).

Real-time reverse-transcription PCR

Real-time reverse-transcription (RT) PCR was performed as described previously.[40] Reaction was subject to one cycle of 95°C for 30 seconds, 45 cycles of PCR at 95°C for 5 seconds, 55°C for 10 seconds, and 72°C for 10 seconds. The following primer pairs were used: 5′-AAGGCCCAGTGTGTCTCTGT-3′ (forward), and 5′-TACCAGCCCCAACTCAAAAC-3′ (reverse) for G-CSF-R, 5′-AGAGGGAAATCGTGCGTGAC-3′ (forward), and 5′-CAATAGTGATGACCTGGCCGT-3′ (reverse) for β-actin, 5′-GCCCCTAGTGCTGCATGAG-3′ (forward) and 5′-CCACAGACACCACATCAATTTCTT-3′ (reverse) for c-Myc.

Western blot analysis

Equal numbers of cells were lysed and Western blotting was performed as described previously.[35,40] Anti-Flag (M2) Ab (Sigma-Aldrich), anti-c-Myc (9E10) Ab (Roche Diagnostics), anti-C/EBPα (14AA) or (N-19) Ab (Santa Cruz Biotechnology), ERK1/2, signal transducer and activator of transcription (STAT)3, STAT5, AKT1, or Flt3 Abs, and phospho-STAT3 Ab (Santa Cruz Biotechnology), anti-phospho mitogen-activated protein kinase and phospho-AKT Abs (Cell Signaling Technology), and phospho-STAT5 Ab (BD Biosciences) were used.

Luciferase assay

The 293T cells were transiently transfected with the luciferase reporter plasmid p(C/EBP)2TK (kindly provided by Atsushi Iwama, Chiba University, Japan), pMXs-C/EBPα-WT or mutants-IP, and pEF-BOS/PU.1 for C/EBPα transcriptional activity, or E2Fx6-TATA-LUC, pCMV-E2F1, and pCMV-DP1 (kindly provided by Claus Nerlov, EMBL Mouse Biology Unit, Italy) for E2F transcriptional activity.[15] Luciferase assays were performed by Dual luciferase assay systems (Promega).

Immunostaining

Immunostaining of 293T cells transiently transfected with retrovirus constructs was performed as described previously.[35] After fixation with 1.5% paraformaldehyde, cells were immunostained with rabbit anti-Flag Ab or fluorescein isothiocyanate–conjugated mouse anti–c-Myc Ab (Sigma-Aldrich). The cells were then stained with Alexa Fluor 546–conjugated goat anti–rabbit immunoglobulin G secondary Ab (Molecular Probes). Nuclei were counterstained with Hoechst (H33342). Fluorescent images were analyzed on a confocal microscope (FLUOVIEW FV300 scanning laser biological microscope JX70 system; Olympus) equipped with SenSys/0L cold charge-coupled device (CCD) camera (Olympus). The objective lens (an LCPlanFl 60×/1.40 NA oil) was used.

Gel shift assay

Nuclear extracts from transfected 293T cells were incubated with 2 μg of polydeoxyinosinic-deoxycytidylic acid and then with double-stranded

Table 1. Clinical features and genetic findings of the patients with *CEBPA* mutations

Patient no.	Age, y/sex	Diagnosis	N terminal C terminal			Karyotype	Other gene mutation*	Survival (years)
			p30 type	bZIP inframe	Frameshift			
MDS/AML								
142	79/F	AML following MDS	I62fsX160	-	-	46,XY[20/20]	-	1.0
829	70/M	AML following MDS	P51fsX160	-	-	45,XY,der(17;18)(q10;q10)[2/20]/46,XY[18/20]	-	0.4
769	69/M	AML following MDS	-	R297P	-	46,XY[20/20]	*AML1, PTPN11*	1.6
896	77/M	AML following MDS	-	K313del	-	46,XY[20/20]	-	0.6
22	71/M	AML following MDS	-	-	G176fsX317	47,XY,+1,der(1;15)(q10;q10)[20/20]	-	0.8
679	89/M	MDS(RAEB)	-	-	P235fsX318	46,XY[20/20]	-	1.9
806	77/M	AML following MDS	G38fsX107	-	R291fsX313	46,XY[20/20]	-	1.9
Therapy-related AML or MDS								
59	80/F	AML(M4)	L19fsX159	-	-	47,XX,+8,t(9;11)(p22;q23)[20/20]	*AML1*	1.7
158	72/F	AML following MDS	F106fsX154	-	-	46,XX[20/20]	-	1.0
811	76/M	MDS(RAEB)	E59X†	-	-	46,XY[20/20]	-	1.7
1068	66/M	MDS(RAEB)	-	Q305P	-	46,XY[20/20]	-	> 1.5
346	59/M	AML following MDS	-	-	S190fsX320	43,XX,del(5)(q31),-7,-15,-18,-21,+mar[20/20]	*N-RAS*	0.8
577	56/F	AML following MDS	-	-	C213X	46,XX[20/20]	-	2.4
629	89/F	AML following MDS	-	-	L350fsX360	46,XX[20/20]	-	1.2
920	69/F	AML(M5)	-	-	S348fsX422	46,XX,t(11;17)(p15;q21)[20/20]	-	0.2
De novo AML(M2)								
40	68/F	AML(M2)	A111fsX166	S299_L304dup	-	46,XX[20/20]	-	> 10.5
292	75/F	AML(M2)	F33fsX107	R297P	-	46,XX[20/20]	-	> 8.4
662	58/F	AML(M2)	S65fsX167	K313dup	-	46,XX[20/20]	-	> 5.0
888	70/F	AML(M2)	A111fsX166	N321D	-	47,XX,+8[20/20]	-	> 3.8
941	31/F	AML(M2Eo)	T60fsX159	304_323dup	-	46,XX,del(7)(q32)[20/20]	-	> 3.5

RAEB indicates refractory anemia with excess blasts.

*Indicates that no mutation was detected in *AML1*, *N-RAS*, *FLT3*, *PTPN11*, *C-KIT*, and *TP53* genes.

†Homozygous mutation.

CSF3R promoter oligonucleotide labeled with γ^{32}P-adenosine triphosphate. Cold competition and a super-shift reaction were carried out by adding a 40-fold excess of cold CSF3R oligo or 1.5 μg of anti-C/EBP (14AA)X Ab (Santa Cruz Biotechnology), respectively. The resulting complexes were resolved on 4.5% polyacrylamide gel.[44]

Colony assay

Infected mouse bone marrow (BM) mononuclear cells (1×10^4) were plated in methylcellulose medium (StemCell Technologies) supplemented with 50 ng/mL each of interleukin (IL)–3, IL-6, stem cell factor, and granulocyte/macrophage-colony-stimulating factor (GM-CSF; R&D Systems) in the presence of 1 μg/mL puromycin. Colonies were counted after 1-week culture, and single-cell suspensions (10^4 cells) of drug-resistant colonies were subsequently replated.

Mouse BMT

Mouse BMT was performed as described previously.[40] Briefly, BM mononuclear cells were isolated from the femurs and tibias of C57BL/6 (Ly-5.1) donor mice 4 days after intraperitoneal administration of 150 mg/kg 5-fluorouracil. The cells were stimulated with 50 ng/mL of mouse stem cell factor, mouse FLT3 ligand, mouse IL-6, and human thrombopoietin (all cytokines were from R&D Systems). The prestimulated cells were infected for 60 hours with the retroviruses harboring pMYs-C/EBPα-C^m-IG, pMYs-C/EBPα-N^m-IG, pMYs-Myc-tagged C/EBPα-C^m-IG, pMYs-Flag-tagged C/EBPα-N^m-IR, pMYs-Flt3-ITD-IG, pMYs-IG, or pMYs-IR, using 6-well dishes coated with RetroNectin (Takara Bio). Then, $3\text{-}5 \times 10^5$ of the infected BM cells (that had not been sorted after either single or double infection) were injected into sublethally γ-irradiated C57BL/6 (Ly-5.2) recipient mice. Overall survival of transplanted mice were estimated using the Kaplan-Meier method. All animal studies were approved by the Animal Care Committee of the Institute of Medical Science, The University of Tokyo.

Statistical analysis

Statistical significance was calculated using the Student *t* test for independent variables. *P* values < .05 were considered statistically significant.

Results

CEBPA mutations in patients with myeloid malignancies

After we performed single-strand conformation polymorphism analysis to screen for *CEBPA* mutations in patients with hematologic disorders, *CEBPA* mutations were identified in 7 of 224 MDS/AML patients, 8 of 71 therapy-related AML or MDS patients, and 5 of 89 de novo AML patients (Table 1). Although the number of the de novo AML patients with *CEBPA* mutations were small, they all carried both an N-terminal mutation and a C-terminal bZIP in-frame mutation on the different alleles as reported previously.[20-26] On the other hand, most MDS/AML or therapy-related AML or MDS patients had single *CEBPA* mutations. As exceptions, we found both an N-terminal mutation and a

C-terminal frame-shift mutation in 1 case of AML after MDS (patient [Pt] #806) and homozygous N-terminal frame-shift mutations in one case of therapy-related MDS/RAEB (Pt #811). Examination of other genes (*RUNX1, N-RAS, FLT3, PTPN11, C-KIT,* and *TP53* gene) in these patients demonstrated that one case of MDS/AML (Pt #769) had both *RUNX1* and *PTPN11* mutations and that patients with therapy-related AML or MDS (Pt #59 or #346) had a mutation of *RUNX1* or of *N-RAS*, respectively. Consistent with recent reports,[22,26] our clinical data showed that overall survival was better in de novo AML patients with double *CEBPA* mutations compared with others with single *CEBPA* mutations (Table 1). These results suggested that double *CEBPA* mutations were able to induce AML, whereas single *CEBPA* mutation would lead to more aggressive AML, in concert with other gene alterations that have not been fully characterized.

The C-terminal but not N-terminal mutations of C/EBPα inhibited G-CSF–induced differentiation of 32Dcl3 cells into mature neutrophils

For further analysis, we chose an N-terminal mutant producing p30 designated as C/EBPα-N^m and a C-terminal b-ZIP in-frame mutant designated as C/EBPα-C^m (Figure 1A). C/EBPα-WT, C/EBPα-N^m, C/EBPα-C^m, C/EBPα-p30, or mock (pMXs-IP) was expressed in Plat-E cells. Expression of p42 protein or p30 protein generated by Myc-tagged C/EBPα-WT and mutants was verified by using anti-Myc Ab as bands corresponding to expected molecular weights (Figure 1B). In addition, we confirmed that N-terminal polypeptide produced by C/EBPα-N^m was detected by anti-C/EBPα Ab recognizing the N-terminal portion of C/EBPα (supplemental Figure 1, available on the *Blood* Web site; see the Supplemental Materials link at the top of the online article). Notably, the expression levels of p30 generated by C/EBPα-N^m were lower than those generated by C/EBPα-p30 (Figure 1B), indicating that deletion of the N-terminal part including the first start codon might increase the expression levels of p30 protein. We then infected 32Dcl3 cells with retroviruses harboring C/EBPα-WT or mutants, and the infected cells were subjected to drug selection. The 32Dcl3 cells expressing detectable levels of C/EBPα-WT were not obtained, presumably due to its strong inhibitory effect on proliferation. Western blot analysis showed that 32Dcl3 cells transduced with C/EBPα-C^m expressed the full length of C/EBPα-C^m at high levels (Figure 1B). C/EBPα-N^m or C/EBPα p30 transduced into 32Dcl3 cells was detected as a band (30 kDa), but the expression level of the former was much lower than that of the latter (Figure 1B). Growth speed was comparable among these transfectants in the presence of IL-3 (Figure 1C). However, the potential of these transfectants to differentiate in response to G-CSF varied; G-CSF treatment induced terminal differentiation of 32Dcl3 cells transduced with mock, as indicated by the appearance of polymorphonucleated neutrophils and up-regulation of CD11b on the surface (Figure 1D-E). G-CSF–induced granulocytic differentiation of 32Dcl3 cells was profoundly inhibited by C/EBPα-C^m, while it was only weakly inhibited by C/EBPα-N^m (Figure 1D-E). The differentiation was also attenuated by C/EBPα-p30, as reported previously.[45] We reasoned that the difference of 32Dcl3 cells expressing C/EBPα-N^m or C/EBPα-p30 in the granulocytic differentiation levels was due to the dissimilar expression levels of a short form of C/EBPα (30 kDa). As for the expression levels of G-CSF-R transcripts, a target of C/EBPα, they were extremely or moderately decreased in 32Dcl3 cells expressing C/EBPα-C^m or C/EBPα-p30, respectively, compared with other transfectants (Figure 1F), implicating G-CSF-R in induction of granulocytic differentiation. However, when human G-CSF-R was transduced into C/EBPα-C^m-expressing 32Dcl3 cells, G-CSF–induced granulocytic differentiation was not completely recovered (supplemental Figure 2). These results indicated that the differentiation block in 32Dcl3 cells expressing C/EBPα-C^m was presumably due to the suppression of C/EBPα activation, but not simply due to the decreased expression of G-CSF-R downstream of C/EBPα.[46]

C/EBPα-C^m or C/EBPα-N^m suppressed the transcriptional activity of C/EBPα-WT by different mechanisms

We next analyzed the transcriptional activation of C/EBPα-WT and mutants in 293T cells using a luciferase construct harboring 2 C/EBPα binding sites. As expected, C/EBPα-WT strongly activated this promoter, while neither C/EBPα-C^m, C/EBPα-N^m, nor C/EBPα-p30 showed any transcriptional activation (Figure 2A). We next examined whether these C/EBPα mutants affected the transcriptional activation of C/EBPα-WT. Although C/EBPα-C^m reduced G-CSF-R expression and inhibited G-CSF–induced myeloid differentiation of 32Dcl3 cells even more efficiently than C/EBPα-N^m (Figure 1D-F), C/EBPα-N^m as well as C/EBPα-p30 but not C/EBPα-C^m decreased promoter activity in the luciferase assay in 293T cells (top panel in Figure 2A), which was in accordance with the data shown by Gombart et al.[20] Expression of C/EBPα WT and mutants in the transfected 293T cells was verified by Western blot analysis (bottom panel in Figure 2A). These results indicated that C/EBPα-C^m and C/EBPα-p30 suppressed expression of G-CSF-R by different mechanisms. Interestingly, transcriptional activation of C/EBPα-WT drastically increased in 293T cells when coexpressed with PU.1, although PU.1 itself did not stimulate the same promoter (top panel in Figure 2B). Notably, this synergistic effect was suppressed by C/EBPα-C^m and weakly by C/EBPα-N^m with low expression levels of p30 protein (top panel in Figure 2B). Expression of C/EBPα and PU.1 was also confirmed by Western blot analysis (bottom panel in Figure 2B). Therefore, we assumed that C/EBPα-C^m was interacting with other transcription factors such as PU.1, thereby suppressing the activation of C/EBPα-WT in hematopoietic cells. We also tested whether the C/EBPα mutants inhibit E2F activity. However, neither C/EBPα-C^m nor C/EBPα-N^m repressed E2F1/DP1-mediated transcription (supplemental Figure 3). In this regard, there was no difference between C/EBPα-C^m and C/EBPα-N^m. We then compared the DNA-binding ability of C/EBPα-WT and mutants by electrophoresis mobility shift assay. As shown in Figure 2C, C/EBPα-WT protein bound to the CSF3R (G-CSF-R) probe, and C/EBPα-p30 protein generated by C/EBPα-N^m less efficiently bound to the same probe. Binding was verified by super-shift of the DNA-protein complex by the anti-C/EBPα Ab. Remarkably, C/EBPα-C^m failed to bind the CSF3R probe (Figure 2C). Next, we examined subcellular localization of C/EBPα-WT and mutants. In line with previous reports, C/EBPα-WT and mutants localized in the nucleus of the interphase cells (Figure 2D). However, it was noteworthy that unlike C/EBPα-WT and C/EBPα-p30, C/EBPα-C^m was not localized on chromosome during the mitotic phase (Figure 2D). It is possible that C/EBPα-C^m without a DNA binding ability is stealing some interacting protein from chromosome. Taken together, these results indicated that C/EBPα-N^m suppressed the transcriptional activation of C/EBPα-WT by its direct binding to the promoter or by its heterodimerization with C/EBPα-WT, while C/EBPα-C^m showed the suppressive effect indirectly, probably through interaction with other transcription factors such as PU.1.

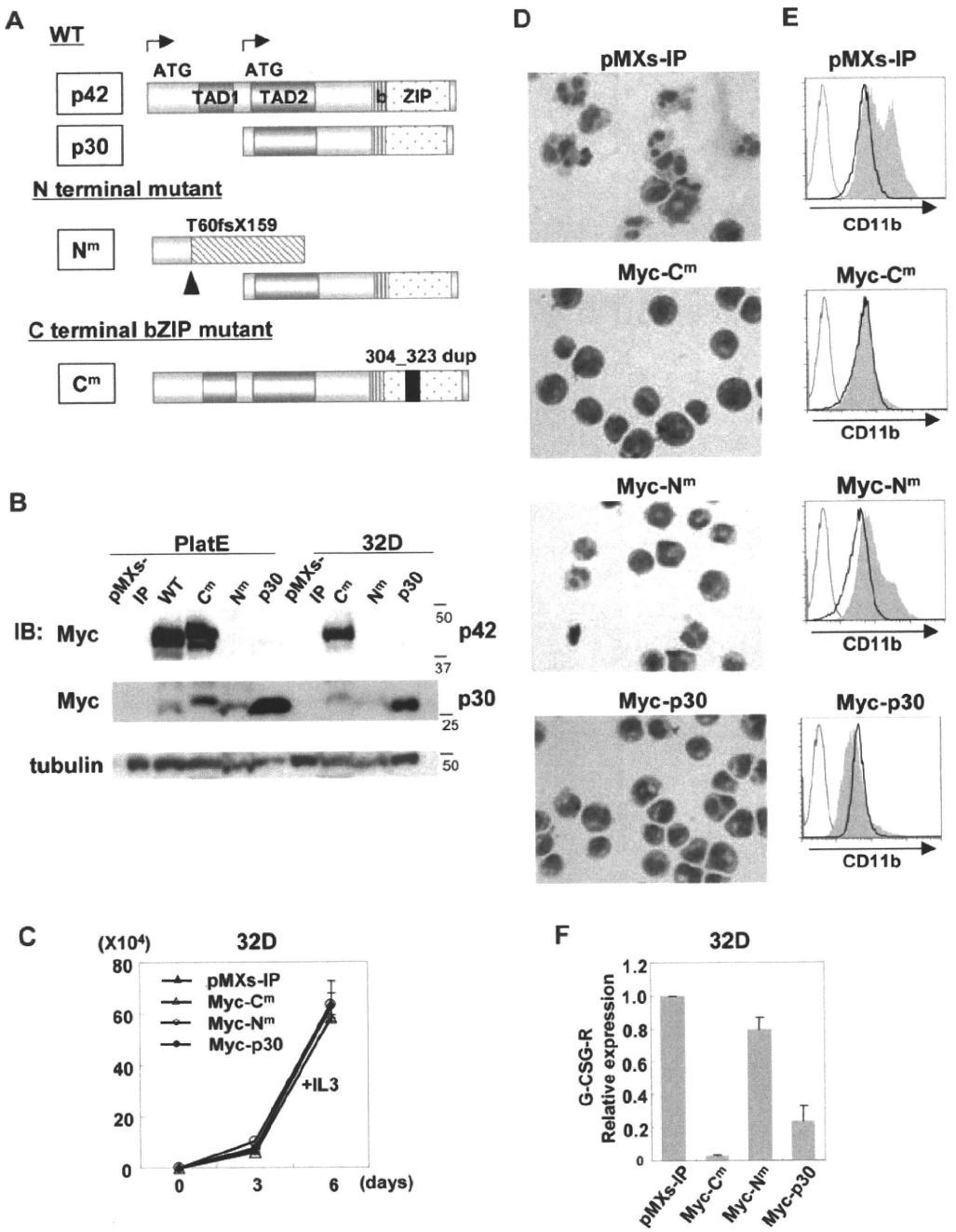

Figure 1. C/EBPα-C^m had the strong ability to block myeloid differentiation. (A) Schematic diagram of C/EBPα-WT (p42 and p30) and mutants, T60fsX159 (C/EBPα-N^m) and 304_323 dup (C/EBPα-C^m). TAD indicates the transcriptional activation domain; bZIP, basic region leucine zipper domain. (B) Expression of C/EBPα-WT and its mutants in Plat-E cells transiently transfected with a Myc-tagged C/EBPα-WT, C/EBPα-C^m, C/EBPα-N^m, or C/EBPα-p30 or an empty vector (pMXs-IP) and expression of C/EBPα mutants in 32Dcl3 cells transduced with Myc-tagged C/EBPα-C^m, C/EBPα-N^m, C/EBPα-p30, or mock (pMXs-IP). Cell lysates were subject to immunoblotting with anti-Myc Ab or anti-tubulin Ab as control. The results shown are representative of 3 independent experiments. (C) The growth of 32Dcl3 cells transduced with Myc-tagged C/EBPα-C^m, C/EBPα-N^m, C/EBPα-p30, or mock (pMXs-IP) in the presence of 1 ng/mL IL-3. All data points correspond to the mean and the standard deviation (SD) of 3 independent experiments. (D-E) 32Dcl3 cells transduced with Myc-tagged C/EBPα-C^m, C/EBPα-N^m, C/EBPα-p30, or mock (pMXs-IP) were cultured in the presence of 50 ng/mL G-CSF for 6 days. (D) Morphology of these cells was assessed by Giemsa staining. Images were obtained with a BX51 microscope and a DP12 camera (Olympus); objective lens, UplanFI (Olympus); original magnification ×40. (E) Surface expression of CD11b in these transfectants after incubation with 1 ng/mL IL-3 (bold histograms) or 50 ng/mL G-CSF (filled histograms) for 6 days was analyzed by flow cytometry. The result of control staining is shown as a thin-lined histogram. Data are representative of 3 independent experiments. (F) Relative expression levels of G-CSF-R in 32Dcl3 cells transduced with Myc-tagged C/EBPα-C^m, C/EBPα-N^m, C/EBPα-p30, or mock (pMXs-IP) were estimated by using real-time PCR. Data are representative of 3 independent experiments.

Retroviral transduction of C/EBPα-C^m, but not C/EBPα-N^m, immortalized BM hematopoietic cells

To determine the effect of C/EBPα-C^m and C/EBPα-N^m on differentiation and proliferation of hematopoietic cells, we performed serial colony-forming assays as described previously.[45] Mouse BM mononuclear cells were transduced with C/EBPα-C^m, C/EBPα-N^m, or C/EBPα-p30. Expression of C/EBPα mutants in the transduced BM cells was verified by Western blot analysis

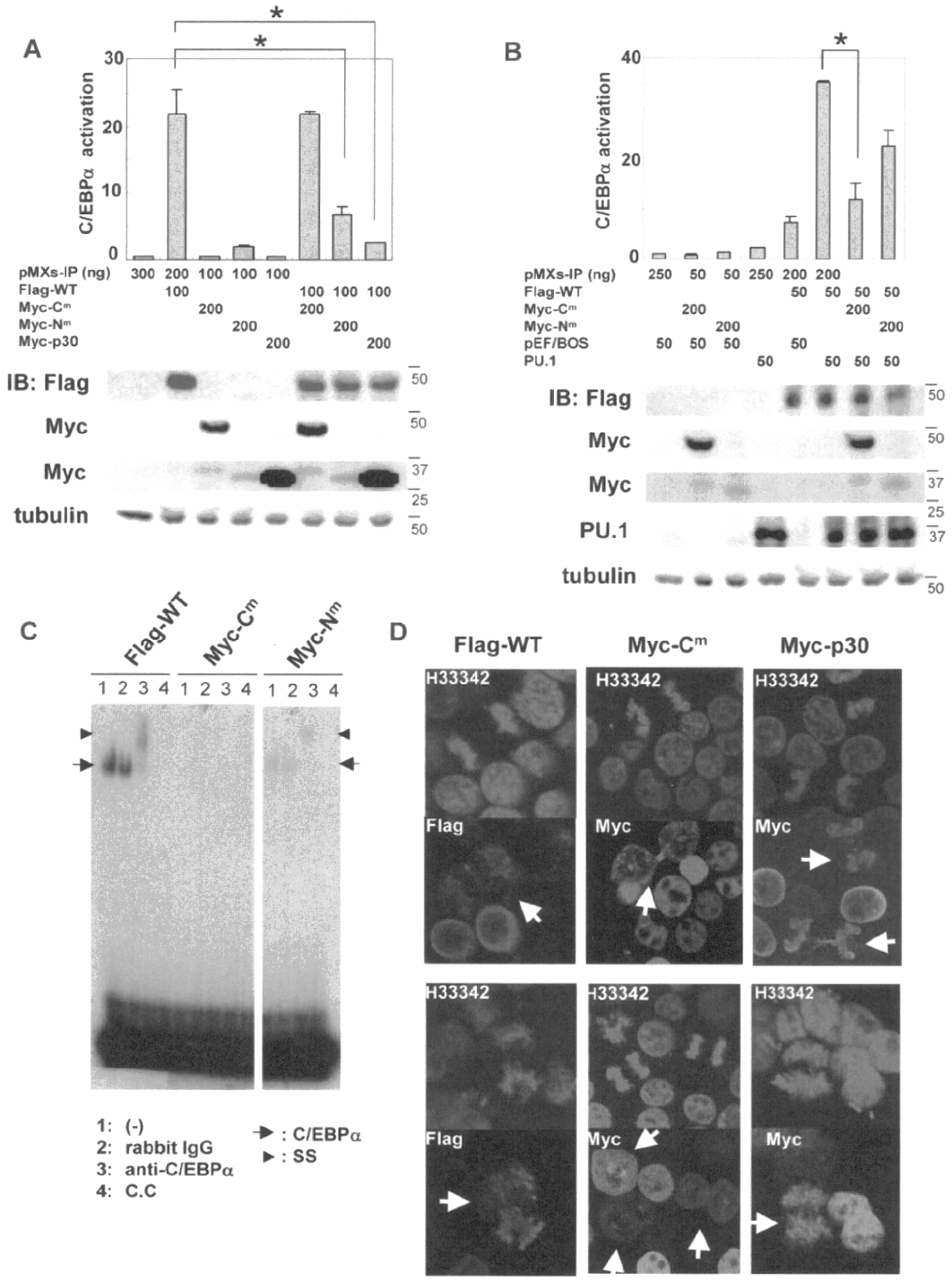

Figure 2. C/EBPα-C^m or C/EBPα-N^m inhibited the transcriptional activation of C/EBPα-WT by different mechanisms. (A-B top) 293T cells were transiently transfected with indicated amounts of expression plasmids (pMXs-Flag-tagged C/EBPα WT-IP, pMXs-Myc-tagged C/EBPα mutants-IP, pMXs-IP, pEF-BOS/PU.1, pEF-BOS) together with 100 ng of the luciferase reporter plasmid p(C/EBP)2TK. The total amount of plasmid for each transfection was adjusted by adding empty plasmids (pMXs-IP or pEF-BOS). Results represented the average values for relative luciferase activity that were normalized using the activity of EF1 vector as an internal control. All transfection groups were normalized with a Renilla luciferase vector as an internal control. All data points correspond to the mean and the standard deviation (SD). Data are representative of 3 independent experiments. Statistically significant differences are shown. *$P < .05$. (Bottom) Expression of C/EBPα-WT, C/EBPα-mutants, or PU.1 in 293T cells transiently transfected as above described. Cell lysates were subject to immunoblotting with anti-Flag Ab, anti-Myc Ab, anti-PU.1 Ab, or anti-tubulin Ab as control. The results shown are representative of 3 independent experiments. (C) DNA binding of C/EBPα-WT and mutants. Electrophoresis mobility shift assay was performed with ^{32}P-labeled oligonucleotides containing the C/EBPα binding site derived from CSF3R promoter and nuclear extracts from 293T cells transiently transfected with pMXs-Flag–tagged C/EBPα WT-IP, pMXs-Myc–tagged C/EBPα-C^m-IP, or pMXs-Myc–tagged C/EBPα-N^m-IP. Data are representative of 3 independent experiments. Lane 1: none (−); lane 2: control rabbit immunoglobulin G was added; lane 3: anti-C/EBPα Ab was added; lane 4: cold competitor (C.C) was added. Ss indicates supershifted bands. (D) 293T cells transiently transfected with pMXs-Flag–tagged C/EBPα-WT-IP, pMXs-Myc-tagged C/EBPα-C^m-IP, or pMXs-Myc–tagged C/EBPα-p30-IP were immunostained with anti-Flag Ab (red) or anti–c-Myc Ab (green) and stained with Hoechst (H33342; blue). Data are representative of 4 independent experiments (total of 15 mitotic cells were examined for each transfectant). Fluorescence images by confocal microscopy were obtained with IX70 (Olympus). Original magnification ×60.

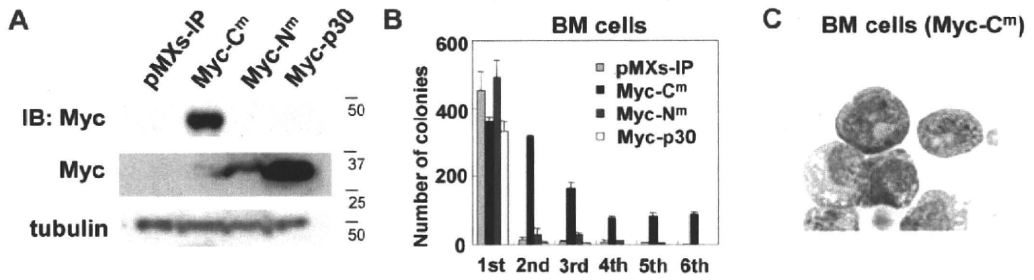

Figure 3. C/EBPα-C^m, but not C/EBPα-N^m, immortalized BM cells. (A) Expression of C/EBPα-C^m, C/EBPα-N^m, or C/EBPα-p30 in BM cells transduced with Myc-tagged C/EBPα-C^m, C/EBPα-N^m, C/EBPα-p30, or mock (pMXs-IP). Cell lysates were subject to immunoblotting with anti-Myc Ab or anti-tubulin Ab as control. The results shown are representative of 3 independent experiments. (B) Colony-forming assay from BM cells transduced with C/EBPα-C^m, C/EBPα-N^m, C/EBPα-p30, or mock (pMXs-IP). Bars represent the number of colonies obtained per 10^4 cells after each round of plating in methylcellulose supplemented with stem cell factor, thrombopoietin, IL-3, and IL-6. Data are representative of 3 independent experiments. All data points correspond to the mean and the standard deviation (SD) of 3 independent experiments. (C) Cytospin preparations of immortalized BM cells transduced with C/EBPα-C^m were stained with Giemsa. Images were obtained with a BX51 microscope and a DP12 camera (Olympus); objective lens, UplanFl (Olympus); original magnification ×100.

(Figure 3A). We also confirmed that the expression levels of p30 protein generated by C/EBPα-p30 are higher than those by C/EBPα-N^m (Figure 3A). Irrespective of different expression levels of p30, most C/EBPα-N^m- and C/EBPα-p30–transduced BM cells did not make secondary colonies after replating (Figure 3B). On the other hand, BM cells expressing C/EBPα-C^m formed colonies after 6 rounds of replating in the presence of cytokine cocktail (Figure 3B). Cytospin preparations of these cells showed blastlike morphologies (Figure 3C). In addition, C/EBPα-C^m–transduced BM cells remained immature and were immortalized in a liquid culture containing IL-3 after several rounds of the replating in semisolid cultures.

Transduction with C/EBPα-C^m into BM cells caused AML in a mouse BMT model

To test whether a single C/EBPα mutant induces hematopoietic abnormality, Ly-5.1 murine BM mononuclear cells, infected with retroviruses harboring C/EBPα-C^m, C/EBPα-N^m, or mock (pMYs-IG), were transplanted into irradiated syngenic Ly-5.2 mice. We confirmed efficient retrovirus infection: 50%-65% of BM cells transduced with C/EBPα-N^m or mock (pMYs-IG) and 35%-50% of BM cells transduced with C/EBPα-C^m were positive for GFP expression before transplantation. Mice receiving transplants of mock (pMYs-IG)–transduced cells (hereafter referred to as mice/pMYs-IG) remained healthy over the observation period (n = 8/8) (Figure 4A). Notably, most of the mice that received transplants of C/EBPα-C^m–transduced cells (hereafter referred to as mice/C^m) developed AML within 4-12 months after transplantation (n = 16/17) (Figure 4A). These morbid mice presented similar phenotypes, characterized by hepatosplenomegaly and pancytopenia (Table 2). BM and spleen were occupied with myeloblasts and myelocytes (Figure 4B). In some cases, leukemic cells displayed morphologic aberrations such as abnormal lobular and ring-shaped nucleus. GFP-positive leukemic cells expressed CD11b and Gr-1 at high levels and c-kit at intermediate to high levels (middle panel in Figure 4C). One of the mice/C^m developed T-cell lymphoma with thymoma (data not shown). We next asked if the integration of retroviruses influenced the outcomes in the BMT model. Southern blot analysis of BM cells of mice/C^m showed a single or several integrations (supplemental Figure 4), and either 1 or 2 integration sites were identified in these samples, based on the inverse PCR method (supplemental Table 1).[47] We found several common integration sites and integrations of the retroviruses in the intron of MN1 in 2 of 15 cases examined (supplemental Table 1). Considering the recent works published by Hasemann et al[48] and by ourselves,[40] retrovirus integration might in part influence the phenotypes of the recipient mice in our BMT models. For example, integration of the retrovirus vector into MN1 may enhance cell growth.[40] However, integration sites do not seem to play major roles in the experiments of this study; C/EBPα-C^m transduction induced AML with similar phenotypes in most cases after a relatively long latency in the BMT model. On the other hand, 5 of 8 mice that received transplants of C/EBPα-N^m–transduced cells (hereafter referred to as mice/N^m) remained healthy during the observation period. Three of 8 mice/N^m developed B-cell acute lymphoblastic leukemia (B-ALL) with hepatosplenomegaly with latencies of 7 to 12 months after transplantation (Figure 4A). BM was occupied with blastlike cells, and the morbid mice exhibited leukocytosis, anemia, and thrombocytopenia (Figure 4B and data not shown). GFP-positive leukemic cells expressed B220 and CD19 at high levels and c-kit at intermediate to high levels (right panel in Figure 4C). One of the mice/N^m developed AML with splenomegaly 13 months after transplantation (data not shown). The reason why C/EBPα-N^m tend to induce B-ALL is not clear. However, we must notice a point that mouse BMT models may not always mimic human diseases.[35,40] Expression of C/EBPα-C^m in spleen cells of mice/C^m with AML or p30 protein generated by C/EBPα-N^m in spleen cells of mice/N^m with B-ALL was confirmed by Western blot analysis (Figure 4D). Collectively, C/EBPα-C^m has a potential to strongly induce AML in a BMT model. Because the latency is relatively long and the leukemic cells seem to be clonal, additional events should have worked with C/EBPα-C^m in inducing leukemia. In addition, the in vivo suppressive effect of C/EBPα-C^m on the activation of endogenous C/EBPα was confirmed by the finding that G-CSF-R expression was down-regulated and c-Myc expression was up-regulated in BM samples of mice/C^m compared with mice/pMYs-IG (Figure 4E-F).

Transduction with both C/EBPα-C^m and C/EBPα-N^m induced more aggressive AML with leucocytosis

To next ask whether the combination of both C/EBPα-C^m and C/EBPα-N^m would induce AML more efficiently, we performed BMT, using murine BM mononuclear cells infected with retroviruses harboring Myc-tagged C/EBPα-C^m-IRES-GFP and Flag-tagged C/EBPα-N^m-IRES-dsRED. BM mononuclear cells expressing both mutants were recognized as GFP- and dsRED-double positive cells, 10%-22% of BM cells before the transplantation. Notably, mice that had received transplants of BM cells expressing both mutants (hereafter referred to as mice/Myc-C^m/Flag-N^m) developed AML with hepatosplenomegaly with shorter latencies

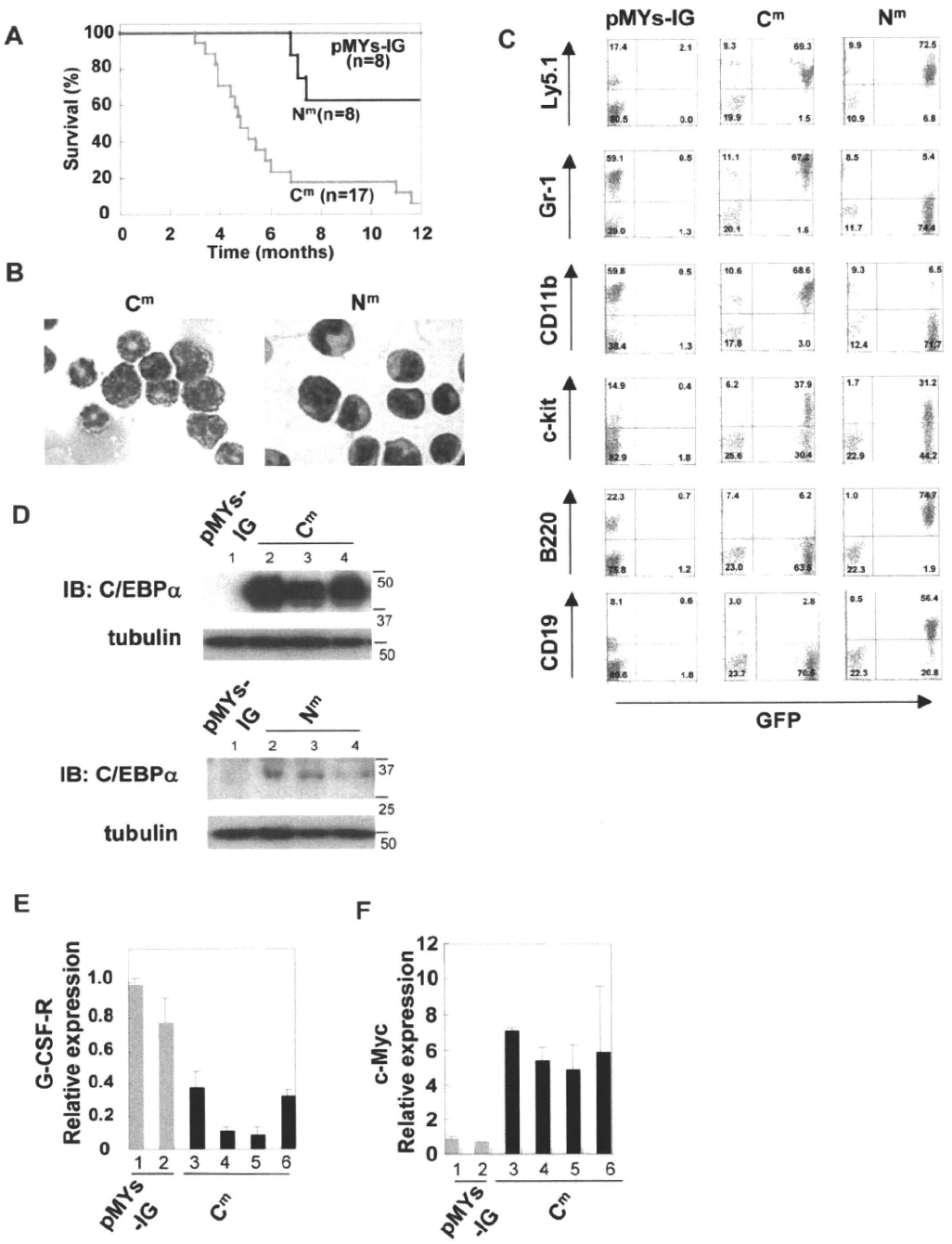

Figure 4. Transduction with C/EBPα-C^m alone induced AML in a mouse BMT model. (A) Kaplan-Meier analysis for the survival of mice that received transplants of BM cells transduced with C/EBPα-C^m-IG (C^m, n = 17), C/EBPα-N^m-IG (N^m, n = 8), or mock (pMYs-IG, n = 8). (B) Cytospin preparations of BM cells derived from mice/C/EBPα-C^m (left) or mice/N^m (right) were stained with Giemsa. A representative photograph is shown. Images were obtained with a BX51 microscope and a DP12 camera (Olympus); objective lens, UplanFl (Olympus); original magnification × 100. (C) Flow cytometric analysis of BM cells derived from mice/C/EBPα-C^m (middle), mice/C/EBPα-N^m (right), or mice/pMYs-IG (left). The dot plots show Ly5.1, Gr-1, CD11b, c-kit, B220, or CD19 labeled with phycoerythrin-conjugated monoclonal Ab versus expression of GFP. (D) Expression of C/EBPα-C^m protein and p30 protein generated by C/EBPα-N^m in spleen cells of mice/pMYs-IG (lane 1) and mice/C^m (lanes 2-4) (top) or in spleen cells of mice/pMYs-IG (lane 1) and mice/N^m (lanes 2-4) (bottom). Cell lysates were subject to immunoblotting with anti-C/EBPα (14AA) Ab or anti-tubulin Ab as control. Data are representative of 3 independent experiments. (E-F) Real-time PCR for G-CSF-R (E) or c-Myc (F) in BM cells derived from mice/C^m or mice/pMYs-IG. Expression levels were normalized by β-actin mRNA. The relative expression level of BM derived from mice/mock (lane 1) was defined as 1. All data points correspond to the mean and the standard deviation (SD) of 3 independent experiments. Lanes 1-2: mice/pMYs-IG; lanes 3-6: mice/C^m.

(3-5 months) compared with mice that had received transplants of BM cells expressing both Myc-C^m-IRES-GFP and mock (pMYs-IR, hereafter referred to as mice/Myc-C^m/pMYs-IR; Figure 5A). Of note, there was no significant difference of the phenotypes between mice/C^m and mice/Myc-C^m/pMYs-IR or between mice/N^m and mice that had received transplants of BM cells expressing both mock (pMYs-IG) and Flag-N^m-IRES-dsRED (hereafter referred to as mice/pMYs-IG/Flag-N^m; Figures 4-5 and data not shown). The percentages of the immature blast ranged from 72%-94% in mice/Myc-C^m/Flag-N^m (Table 2) compared with 62%-92% in